NTNU – Trondheim
Norwegian University of
Science and Technology

Nonlinear Acoustic Waves in Heterogeneous Materials

Adrian Kirkeby

Master of Science in Physics and Mathematics
Submission date: August 2015
Supervisor: Ulrik Skre Fjordholm, MATH
Co-supervisor: Bjørn Atle Angelsen, ISB

Norwegian University of Science and Technology
Department of Mathematical Sciences

Abstract

This thesis concerns the partial differential equations governing acoustic wave propagation in heterogeneous materials. We start with an investigation of the standard Eulerian formulation of the equations, and point out why some of the underlying assumptions and approximations might give inaccurate results in some cases. We argue that a Lagrangian framework is better suited to accurately model wave propagation in materials with discontinuous material properties, and derive a momentum equation in Lagrangian coordinates without approximations. We continue by looking at conservation of energy and attenuation of the wave. To solve the Lagrangian equations on a computer, we propose a numerical scheme based on a Leapfrog on staggered grid-scheme that is second order both in space and time. We also do a numerical experiment and compare results from simulations with the Eulerian and Lagrangian equations. The simulations indicate that the Lagrangian equations are better suited model to certain phenomena.

Sammendrag

Denne oppgaven omhandler differensiallikningene som beskriver oppførselen til akustiske bølger i heterogene materialer. Vi undersøker den klassiske Euler-formuleringen av disse likningene, og peker på hvordan noen av antagelsene og tilnærmingene som gjøres kan være unøyaktige i visse tilfeller. Videre argumenterer vi for hvorfor en Lagrange beskrivelse kan være bedre egnet som en nøyaktig modell av bølgeforplanting i heterogene materialer, og vi utleder en momentlikning i Lagrange-koordinater uten noen antagelser. Vi fortsetter med å se på energibevaring og energitap for akustiske bølger. For å løse Lagrange-likningene numerisk foreslår vi en numerisk metode basert på Leapfrog på staggered grid-metoden, som er andreordens både i tid og rom. Vi gjør et eksperiment med denne metoden, og sammenlikner resultatene fra Euler- og Lagrange-likningene. Resultatene indikerer at Lagrange-likningene er bedre egnet til modellering av visse fenomener.

Takk til

Takk til min familie og mine venner! Spesielt takk til Mamma og Pappa. Og Ola, Terje, Marte, Tomas, Johan, Marie og alle andre jeg har bodd og hengt med de siste årene, og til Gaute, Sigbjørn, Sondre og Trygve, til Eline for at du kom på besøk i sommer, og til alle i bandet Trondheim Kommune, til Ulrik for utmerket veiledning, til Bjørn for gode ideer, hjelp og inspirasjon, og til Ola Myhre for tips og triks, og til dere jeg har fått poser under øynene med på datasalen de siste fem årene, og alle andre som har vært til hjelp med skrivingen av denne oppgaven. Og takk til bestefar. Takk!

Contents

Abstract i
Sammendrag i
Takk til ii

Chapter 1. Introduction 1
The Chapters 2
Note on the structure and style of this thesis 2

Chapter 2. Acoustic modeling 3
2.1. Derivation of the acoustic wave equations 4
The linear equations 4
Particle representations 5
The nonlinear equations 5
The Lagrangian density 7
$\mathcal{L}(\mathbf{x}, \mathbf{t}) \approx \mathbf{0}$ 8
A problem with the derivation of the continuity equation 10
Particles represented as a variation in material parameters 11

Chapter 3. Lagrangian formulation of the governing equations 13
3.1. Mathematical formulation 13
φ as a mapping 15
3.2. Conservation of mass 15
3.3. Conservation of momentum 17
Nanson's formula 17
The Lagrangian momentum equation 18
The Piola-Kirchhoff stress tensor 18
3.4. An evolution equation for the pressure 20
The acoustic assumption 20
Angelsen's equation 21
A different approach 22

Chapter 4. Energy, viscoelasticity and attenuation 25
4.1. Conservation of Energy 25
Acoustic intensity and Power 26
Energy conservation for the Lagranigan equations 28
4.2. Viscoelasticity and attenuation 28
The Three-element-model 30
Frequency dependent attenuation 32

Chapter 5. Numerical Method 33
5.1. Sources 33
5.2. Split-field Perfectly Matched Layer 35
5.3. Discretization 39
Leapfrog on Staggered Grid for the Eulerian equations 39
Leapfrog on Staggerd Grid for the Lagrangian equations 42

Properties of the scheme 46
Implementation 47

Chapter 6. Numerical experiment 49
6.1. The experiment 49
Summary and further work 56

Appendix 57

Bibliography 63

CHAPTER 1

Introduction

The understanding of waves is fundamental to our of understanding the physical world. Waves are present at the largest and the smallest scales of the universe, from cosmic rays and tsunamis to quantum physics and vacuum fluctuations in outer space. A scientific understanding of waves has been a concern for scientist since antiquity [15]. As with most physical phenomena, the road to enlightenment goes through experiments and mathematical theories. The mathematical treatment of waves often starts with the derivation of the linear wave equation for transverse waves on a string,

$$\frac{\partial^2 y}{\partial t^2} = c_0^2 \frac{\partial^2 y}{\partial x^2}, \tag{1.1}$$

and this is somehow the canonical example of a wave equation, the one wave equation every student recognizes. Equations of the same form arise in many different areas of physics, from electromagnetics to elasticity.
The linear wave equation serves as a good example of the problems addressed in this thesis. When formulating a mathematical model of a physical problem, one always has to make some simplifying assumptions. The key then, is to make assumptions such that the important features of the physical phenomenon are not lost. If one does not simplify, the mathematical model can become very complex and to hard to analyze. A balance has to be found, where the mathematics is tractable and the physics of interest is modeled adequately. Equation (1.1) serves as an example. The linear wave equation arises when one wants model the propagation of a wave on a string. When deriving it one assumes that certain quantities are small and that there is no loss of energy [31]. If you are interested in understanding the basics of harmonics and vibrations in a string, the equation is very good. It is easy to analyze mathematically, and the solutions shed much light on the physics. If, however, this is a guitar string, and one want to know how long the tone from a plucked string lasts, this model is not good as the equation does not account for loss of energy. Or if you want to know what happens when your guitar makes a "twangy" sound just as you pluck the string; this is a nonlinear effect, not accounted for in this equation [12]. This illustrates that when you make a mathematical model of a physical phenomenon, you have to know, or at least have some notion of, what is essential for describing the phenomenon of interest.

In this thesis we are interested in acoustic waves. Simply told, acoustic waves, commonly known as sound waves, are waves that propagate as local compression and expansion of the medium they travel through. More specifically, we are interested in ultrasonic waves propagation in the human body in interaction with very small[1] objects. Ultrasonic waves are acoustic waves with frequencies higher than the upper range of what is audible for humans, i.e. in the range 20 kilohertz to 40 megahertz. One usage of these waves is in in medical imaging, where it is a common tool for "looking" inside the body, and also for treatment. This is a broad field of study and research, widely known as ultrasound. We want to look at one particular aspect of ultrasound, namely the equations used to model it. What are the underlying assumptions made in the standard equations used in acoustic wave models, and what are the assumptions in these equations? By the initiative of prof. *Bjørn A. J. Angelsen* at ISB[2], we investigate

[1] Objects on the same scale as the wavelength.

[2] Department of Circulation and Medical Imaging at NTNU

how a Lagrangian formulation of the equations would look, in contrast to the commonly used Eulerian formulation. As we will see, the Lagrangian formulation of the equations seems to be more suited to model the interaction between ultrasonic waves and microscopic structures, e.g. calcium particles or micro bubbles. We also develop a numerical method for solving the Lagrangian equations. An extension of this work is in connection with SURF Technologies and their research on using ultrasound to detect breast cancer. An early sign of breast cancer is clusters of micro calcium particles in the breast. Due to their tinyness (20-300 μm in diameter), these are very hard to detect. If their interaction with high intensity ultrasonic waves is properly understood, one might come closer to finding a way to discover them.

The Chapters

- Chapter 1 is the introduction.

- Chapter 2 discusses the standard, Eulerian formulation of the equations governing propagation of acoustic waves, and ways to represent heterogeneities in these equations. We point out how certain approximations made in the derivation of these equations can lead to inaccurate results.

- Chapter 3 concerns the formulation of the Lagrangian equations governing wave propagation. We introduce the Lagrangian description of the continuum, and use this framework to develop a different set of governing equations.

- Chapter 4 addresses conservation of energy in acoustic waves, and show how a viscoelastic model can be added to the Lagrangian equations to account for the attenuation of energy.

- Chapter 5 describes a numerical method for solving the equations developed in Chapter 4. We add a PML damping layer, sources and other necessary conditions, and propose a numerical scheme to solve the first order system of Lagrangian equations.

- Chapter 6 describes a numerical experiment using the scheme from Chapter 5. We look at the reflection of intersecting waves from a calcium particle, and compare results from the Lagrangian and Eulerian equations.

Note on the structure and style of this thesis

As the discussion on the different topics in this text overlap to some extent, some concepts might be introduced and discussed before they are properly defined and described. However, we aim to give an adequate description of the important topics when needed. Also, the writer has a limited knowledge to the wast field of ultrasound, and the thesis probably reflects this. It is written from the perspective of a mathematician, with focus on some particular equations, and the writer most definitely have the feeling of being a beginner.

CHAPTER 2

Acoustic modeling

We now introduce quantities and equations[1] used to describe acoustic waves. We also look at how one could represent particles and material heterogeneity in the Eulerian[2] framework commonly used in acoustic modeling, and point out how some of the assumptions and simplifications that can cause the equations to not adequately model the interaction of waves and small particles and heterogeneities.

The main quantities in the description of a wave propagation are:

- Acoustic pressure: $p(x,t) = P(x,t) - P_0$
  The acoustic pressure is deviation of total pressure $P(x,t)$ from the static, or ambient, pressure P_0. Pressure is a scalar quantity.
- Particle velocity: $v(x,t) = V(x,t) - V_0$
  This is the time derivative of the particle displacement, and V_0 is usually assumed equal to zero. Velocity is a vector quantity.
- Mass density: $\rho'(x,t) = \rho(x,t) - \rho_0(x)$
  ρ' is the excess mass density, or mass per unit volume, a scalar quantity. Mass density is closely connected to the acoustic pressure and the compression and expansion of the material. ρ is the total density, while ρ_0 is the ambient, or equilibrium density.
- Compressibility: κ
  Compressibility is a measure of volume compression due to change in pressure. We denote the equilibrium density as κ_0. κ_0 (and ρ_0) are material dependent parameters, we will refer to them as material parameters.
- Sound speed: c
  The sound speed is the speed at which an acoustic wave propagates through a material. At equilibrium we denote $c = c_0$, and we have the relation $c_0^2 = \frac{1}{\kappa_0 \rho_0}$

Most formulations of the acoustic equations begin with two well-known conservation laws, and what is known as an equation of state. A derivation of the conservation laws can e.g. be found in [8, 4], and we will comment on it later. The first equation, often known as the continuity equation, is a mathematical description of the principle that mass is conserved,

$$\frac{\partial \rho}{\partial t} + \nabla \cdot (\rho v) = 0. \tag{2.1}$$

[1] Most of the time, equations means partial differential equations.

[2] We will elaborate on the Eulerian and Lagrangian descriptions later.

The second equation is known as conservation of momentum, and is essentially Newton's second law. It reads

$$\rho \frac{\mathrm{D}v}{\mathrm{d}t} = -\nabla p, \tag{2.2}$$

where $\frac{\mathrm{D}}{\mathrm{d}t} = \frac{\partial}{\partial t} + v \cdot \nabla$ is known as the total or material derivative. To connect the equations and get a complete system, one introduces a relation between the density and pressure. This is called an equation of state, generically written $p = P(\rho)$. It is material dependent, and will later be specified.

2.1. Derivation of the acoustic wave equations

At this point it is informative to do the standard derivation of the governing equations, as it is presented in the literature [15, 31, 10]. It will become more apparent why the standard approach is not well suited for an accurate description of the behavior and wave interaction of a particle.

The linear equations

In a derivation of the acoustic wave equation(s), it is usual to decide on what order of accuracy one wants. First order means you only include first order terms. First order terms are linear terms, e.g. $\frac{\partial^2 p}{\partial t^2}$, v, etc., second order means term on the form p^2, vp, $\frac{\partial v}{\partial t} v$ etc. We start with the linear equations, where we include only first order terms of the acoustic quantities. The linear equation of state is

$$p = c_0^2(\rho'), \tag{2.3}$$

that is, the acoustic pressure p is equal to the excess density ρ' times the squared speed of sound c_0^2 [15]. From (2.1), we get

$$\frac{\partial \rho}{\partial t} + \nabla \cdot (\rho v) = \frac{\partial \rho'}{\partial t} + \nabla \cdot (\rho' v) + \nabla \cdot (\rho_0 v) \approx \frac{\partial \rho'}{\partial t} + \nabla \cdot (\rho_0 v) = 0, \tag{2.4}$$

where the last transition is from neglecting the second order term $\nabla \cdot (\rho' v)$. By inserting (2.3) and assuming that the ambient density[3] ρ_0 is constant, one obtains an equation for the pressure:

$$\frac{\partial p}{\partial t} = -c_0^2 \rho_0 \nabla \cdot v \tag{2.5}$$

Linearising (2.2) accordingly yields

$$\rho_0 \frac{\partial v}{\partial t} = -\nabla p, \tag{2.6}$$

Also assuming c_0 is constant, and combining the temporal derivative of (2.4) and the divergence of (2.6) gives us the familiar

$$\frac{\partial^2 p}{\partial t^2} = c_0^2 \nabla^2 p, \tag{2.7}$$

where $\nabla^2 = \Delta = \nabla \cdot \nabla$ is the divergence of the gradient, known as the Laplace operator. This is the linear acoustic wave equation, and it serves as a good model for the lossless propagation of small-signal waves. Small-signal waves are waves with sufficiently small pressure and velocity amplitudes, s.t. nonlinear effects can be neglected [31]. However, due to the assumption

[3] From the standard derivation as given at `https://en.wikipedia.org/wiki/Acoustic_wave_equation` *"Rearranging and noting that ambient density does not change with time or position..."*

of constant material parameters ρ_0 and c_0, it only describes the propagation in homogenous materials. We now elaborate on how the behavior of the wave in a heterogeneous material is modeled.

Particle representations

A common way of adding the effect of wave-particle interaction to equation (2.7) is through the addition of a source term. Say a particle occupies a small region Ω_p of the material: then there is a change in material parameters ρ_0 and κ_0, and hence, speed of sound inside Ω_p. We define c_p to be the sound speed in Ω_p, and write (2.7) as

$$\frac{1}{c_0^2}\frac{\partial^2 p}{\partial t^2} - \nabla^2 p = -S_p \tag{2.8}$$

where the source term S_p is defined as

$$S_p(x,t) = \begin{cases} \left(\frac{1}{c_0^2} - \frac{1}{c_p^2}\right)\frac{\partial^2 p}{\partial t^2} & \text{for } x \in \Omega_p \\ 0 & \text{for } x \notin \Omega_p \end{cases} \tag{2.9}$$

This approach produces the effects of refraction[4] and reflection, but the method has an ad hoc feel to it, since one reintroduces the varying material parameters after the derivation of the equation where it has been assumed constant. When $c_0 \neq c_p$, it implies discontinuous variation in ρ_0 and κ_0, and the derivation of equation (2.7) would not be justified. Another effect that is not accounted for in this approach is the fact that the wave might exert a force on the particle, causing it to move in space. Such behavior is not accounted for by representing the particle as a static region Ω_p. Another approach is to model Ω_p as a distinct region, with a boundary $\partial\Omega_p$ between it and the surrounding material. This requires the specification of boundary conditions on v and p at $\partial\Omega_p$, and becomes increasingly complex if, in addition, the particle is moving. *Verweij et al.* briefly mention that spatially varying material parameters are important [31], but do not treat it in any detail.

The nonlinear equations

The nonlinear equations rely on the same assumption on material parameters as the linear versions, and particle interaction and homogeneity are modeled accordingly. Nonlinear effects are important in the analysis and use of ultrasound [8, 10]. The justification of linearization relies on the assumption that signals are sufficiently small, but this is not always the case. When signals are large, nonlinear effects must be accounted for to give an adequate description of wave propagation.

By nonlinear equations, we mean nonlinear up to second order. The derivation of these equations use a principle called "repeated substitution", which says that you can substitute relations from the linear equations into the nonlinear relations.[5] Details of the derivations can be found

[4] Refraction is the change of propagation direction due to heterogeneity.

[5] This is justified by the fact that substitution of higher order equations would introduce quantities of order > 2, which again would have to be neglected.

in [10], but roughly it goes like this: We expand the continuity equation (2.1)

$$\frac{\partial \rho'}{\partial t} + \rho_0 \nabla \cdot v + \rho' \nabla \cdot v + v \cdot \nabla \rho' = 0. \tag{2.10}$$

Now we use the linear equation of state (2.3),

$$\frac{\partial \rho'}{\partial t} + \rho_0 \nabla \cdot v = -\frac{p}{c_0^2} \nabla \cdot v - \frac{v}{c_0^2} \cdot \nabla p, \tag{2.11}$$

and substitution of the linear relations from (2.4) and (2.6), to get

$$\frac{\partial \rho'}{\partial t} + \rho_0 \nabla \cdot v = \frac{p}{\rho_0 c_0^4} \frac{\partial p}{\partial t} + \frac{\rho_0 v}{c_0^2} \cdot \frac{\partial v}{\partial t}. \tag{2.12}$$

At this point one introduces the Lagrangian density $\mathcal{L}(x,t) = \frac{1}{2}\rho_0 v^2 - \frac{1}{2}\kappa_0 p^2$, where $\kappa_0 = \frac{1}{\rho_0 c_0^2}$ and $v^2 = v \cdot v$. We will return to the Lagrangian density later. If we include $\mathcal{L}(x,t)$ and divide by ρ_0 we get

$$\frac{1}{\rho_0} \frac{\partial \rho'}{\partial t} - \kappa_0^2 \frac{\partial p^2}{\partial t} = -\nabla \cdot v + \kappa_0 \frac{\partial}{\partial t} \mathcal{L}(x,t) \tag{2.13}$$

Now one could subtitute $\rho' = \frac{1}{c_0^2} p$ and have a nonlinear PDE for the pressure. Nonlinearity is however, a material dependent property, and this is captured by the nonlinear equation of state,

$$\rho' = \frac{1}{c_0^2} p - \frac{1}{\rho_0 c_0^4} \frac{B}{2A} p^2 \qquad \text{or} \qquad \frac{\rho'}{\rho_0} = \kappa_0 p - \kappa_0^2 \frac{B}{2A} p^2. \tag{2.14}$$

The relation is obtained by second order Taylor expansion of the generic relation $p = P(\rho)$, around ρ_0 [10]. A and B are material specific parameters, given as

$$A = \rho_0 \left(\frac{\partial p}{\partial \rho} \right)_{s,0} = \rho_0 c_0^2$$
$$B = \rho_0^2 \left(\frac{\partial^2 p}{\partial \rho^2} \right)_{s,0},$$

where the subscript $(s,0)$ indicates that the partial derivatives are evaluated for constant entropy, i.e. that there is an assumption of no extrinsic or intrinsic heat loss in the process [4]. Measured values of $\frac{B}{A}$ exist for a range of materials [31]. As *Robert T. Beyer* writes in [15], *"... [the parameter $\frac{B}{A}$] characterizes the dominant finite amplitude contribution to the sound speed for an arbitrary fluid."* Hence (2.14) should be used for a more accurate description of nonlinear effects. Substitution of the nonlinear equation of state in to (2.13) yields

$$\frac{\partial}{\partial t} \left(\kappa_0 p - \beta \kappa_0^2 p^2 \right) = -\nabla \cdot v + \kappa_0 \frac{\partial}{\partial t} \mathcal{L}(x,t), \qquad \text{where} \qquad \beta = 1 + \frac{B}{2A}. \tag{2.15}$$

The parameter β is commonly used in acoustics, and accounts for both the inherent and material specific nonlinearity. The inherent nonlinearity is present in all waves, accounted for by the factor 1 in β. Material specific nonlinearity, represented by $\frac{B}{2A}$, are nonlinear effects that occur due to the structure of the material. Hence, all waves are nonlinear, but how much depends on the material.

When deriving the nonlinear equation for conservation of momentum, a similar approach is followed, with the additional assumption that the velocity field is irrotational, i.e. that $\nabla \times v = 0$.

This can be thought of as a linear approximation: A result from vector calculus says that for any scalar field, e.g. the acoustic pressure field p, $\nabla \times \nabla p = 0$ [2]. Applying this to equation (2.6) we get

$$\nabla \times \left(\rho_0 \frac{\partial v}{\partial t} \right) = -\nabla \times \nabla p = 0 \quad \Longrightarrow \quad \rho_0 \frac{\partial}{\partial t} (\nabla \times v) = 0 \quad \Longrightarrow \quad \nabla \times v = 0.$$

By using the identity $v \cdot \nabla v = \frac{1}{2} \nabla v^2 - v \times (\nabla \times v)$ we can rewrite the nonlinear term in the total derivative:

$$\frac{\mathrm{D}v}{\mathrm{d}t} = \frac{\partial v}{\partial t} + \frac{1}{2} \nabla (v^2) - v \times (\nabla \times v) = \frac{\partial v}{\partial t} + \frac{1}{2} \nabla v^2 \tag{2.16}$$

By following a similar procedure as above, we get the nonlinear equation for conservation of momentum:

$$\begin{aligned} \rho \frac{\mathrm{D}v}{\mathrm{d}t} &= (\rho_0 + \rho') \frac{\partial v}{\partial t} + (\rho_0 + \rho') \frac{1}{2} \nabla v^2 \\ &\approx \rho_0 \frac{\partial v}{\partial t} + \rho_0 \frac{1}{2} \nabla v^2 + \rho' \frac{\partial v}{\partial t} \\ &\approx \rho_0 \frac{\partial v}{\partial t} + \rho_0 \frac{1}{2} \nabla v^2 - \kappa_0 p \nabla p \end{aligned}$$

Including the pressure gradient and rearranging we get

$$\rho_0 \frac{\partial v}{\partial t} = -\nabla p - \nabla \mathcal{L}(x,t) \tag{2.17}$$

Once again, the Lagrangian density $\mathcal{L}$ appears. We now take a closer look at the role of the Lagrangian density in acoustic models.

The Lagrangian density

The Lagrangian density appears in both (2.17) and (2.15). It has its name from the theory of Lagrangian mechanics, where it serves as a important tool for obtaining the governing differential equations, through the principle of stationary action [11]. The Lagrangian is defined as $L = K - V$, where K and V are the total kinetic and potential energy of the system. Hence, in our case L would be

$$L = \int \mathcal{L} \mathrm{d}V = \int \frac{1}{2} \rho_0 v^2 - \frac{1}{2} \kappa_0 p^2 \mathrm{d}V \tag{2.18}$$

It is well known that the kinetic energy density is $\varepsilon_K = \frac{1}{2} \rho v^2$, and in acoustics the potential energy density of a wave is sometimes defined as $\varepsilon_P = \frac{1}{2} \kappa_0 p^2$ [8], although there seems to be different opinions on this [28]. We will later show that a different expression for ε_P is needed for nonlinear waves. However, the main point about the Lagrangian density is not if it is correct in terms of representing the kinetic and potential energy, but that for it can be neglected. This might seem dramatic, but the reason lies in the fact that it does not contribute to cumulative nonlinear effects in the wave propagation, since $\mathcal{L}(x,t) \approx 0$ after a very short propagation distance. Cumulative nonlinear effects are effects that occur due to variation in propagation speed along the wave form, i.e. because the wave is influencing its own wave speed, an effect that can cause development of shocks [15]. We now show why $\mathcal{L}$ can be neglected when one only concerns cumulative nonlinearity.

$$\mathcal{L}(\mathbf{x},\mathbf{t}) \approx \mathbf{0}$$

In the case of a wave originating from a point source in $\mathbb{R}^3$, the homogenous, linear wave equations reduces to a one dimensional equation in the following way: Let $r = ||x|| = \sqrt{x^2+y^2+z^2}$. Due to symmetry of the spherical waves from a monopole point source, i.e. a small, vibrating sphere that expands and compresses the material equally in all directions [31], the Laplace operator only has a radial part [7]:

$$\nabla^2\phi(r,t) = \frac{1}{r^2}\frac{\partial}{\partial r}\left(r^2\frac{\partial\phi(r,t)}{\partial r}\right) = \frac{\partial^2\phi(r,t)}{\partial r^2} + \frac{2}{r}\frac{\partial\phi(r,t)}{\partial r} = \frac{1}{r}\frac{\partial^2}{\partial r^2}(r\phi(r,t)). \tag{2.19}$$

Still assuming the velocity is irrotational, we introduce the velocity potential ϕ. It is defined as

$$\nabla\phi = v. \tag{2.20}$$

The governing equations is as before

$$\kappa_0\frac{\partial p}{\partial t} + \nabla\cdot v = 0 \tag{2.21}$$

$$\rho_0\frac{\partial v}{\partial t} + \nabla p = 0. \tag{2.22}$$

Combing (2.21),(2.22) and (2.20), we get a wave equation for ϕ and a simple relation between p and ϕ

$$\frac{\partial^2\phi}{\partial t^2} = c_0^2\nabla^2\phi \quad \text{and} \quad p = -\rho_0\frac{\partial\phi}{\partial t} \tag{2.23}$$

and the wave equation for the potential in spherical coordinates becomes

$$\frac{\partial^2\phi}{\partial t^2} = \frac{c_0^2}{r}\frac{\partial^2}{\partial r^2}(r\phi), \quad \text{or} \quad \frac{\partial^2}{\partial t^2}(r\phi) = c_0^2\frac{\partial^2}{\partial r^2}(r\phi). \tag{2.24}$$

We now have a 1-D wave equation for $w = r\phi$, and the solution can be computed by d'Alembert's formula. We want to find the solution in the case of a small, vibrating sphere placed at the origin.

The radial position of the sphere boundary is $R(t) = r_0 + r(t)$, where r_0 is some mean position, and $r(t)$ is the boundary oscillations around r_0 with frequency ω. When assuming $|r(t)| << r_0$, we can choose $r(t)$ such that the velocity potential at the boundary is $\phi|_{r_0} = A\sin(\omega t)$, where ω is the angular frequency of the vibration[7]. The solution of (2.24) is of the form

$$\phi(r,t) = \frac{f(r-c_0t)}{r} + \frac{g(r+c_0t)}{r}, \tag{2.25}$$

where f represents an outgoing wave (from the origin) and g represents an incoming wave. Since the sphere is the only source, we only need the f term. We apply the boundary condition to get

$$A\sin(\omega t) = \phi(r_0,t) = \frac{f(r_0-c_0t)}{r_0}. \tag{2.26}$$

Replacing t by $(\frac{r_0}{c_0} - \frac{r}{c_0} + t)$, we have $f(r-c_0t) = r_0A\sin\left(\omega t - \frac{\omega}{c_0}(r-r_0)\right)$, and we get the solution for $\phi(r,t)$:

$$\phi(r,t) = \frac{Ar_0}{r}\sin\left(\omega t - \frac{\omega}{c_0}(r-r_0)\right). \tag{2.27}$$

Using the relation $\frac{2\pi}{\lambda} = \frac{\omega}{c_0}$, where λ is the wavelength, we write

$$\phi(r,t) = \frac{Ar_0}{r}\mathrm{Im}e^{i(\omega t - \frac{2\pi}{\lambda}(r-r_0))}. \tag{2.28}$$

Utilizing the relations between ϕ, p and v in (2.20) and (2.23), remembering that $\nabla = \frac{\partial}{\partial r}\mathbf{e}_r$ due to the symmetry, we have

$$v = -i\frac{2\pi}{\lambda}\left(1 + \frac{\lambda}{i2\pi r}\right)\phi \quad \text{and} \quad p = -i\omega\rho_0\phi \tag{2.29}$$

We now introduce the acoustic impedance, defined as $Z = \frac{p}{v}$. Acoustic impedance is a way to measure a material's resistance to acoustic propagation, and as we will see, it becomes approximately constant. Returning to the wave from the pulsating sphere, we get

$$Z = \frac{p}{v} = \frac{c_0\rho_0}{1 + \frac{\lambda}{i2\pi r}} = c_0\rho_0\left(\frac{1}{1 + \frac{\lambda}{i2\pi||x||}}\right). \tag{2.30}$$

Hence, if $||x|| \gg \lambda$, we see that $Z \approx c_0\rho_0$, i.e. as the wave gets far enough from the source at r_0, the impedance is approximately constant. Rearranging the impedance relation $Z = \frac{p}{v}$, we get

$$v = \frac{p}{Z} \approx \frac{p}{c_0\rho_0} \quad \text{for} \quad ||x|| \gg \lambda \tag{2.31}$$

Returning to the Lagrangian density once again, $\mathcal{L}(x,t) = \frac{1}{2}\rho_0 v^2 - \frac{1}{2}\kappa_0 p^2$, remembering that $\kappa_0 = \frac{1}{c_0^2\rho_0}$, we substitute the relation (2.31) for v:

$$\mathcal{L}(x,t) \approx \frac{1}{2}\rho_0\frac{p^2}{c_0^2\rho_0^2} - \frac{\kappa_0}{2}p^2 = \frac{1}{2}\left(\kappa_0 p^2 - \kappa_0 p^2\right) = 0 \quad \text{for} \quad ||x|| \gg \lambda. \tag{2.32}$$

In [1] *Aanonsen et al.* explain:
"... the $\mathcal{L}$ terms can only produce local effects in the wave solution. They cannot, for a progressive wave, lead to cumulative effects. These are fully accounted for through the $\left[q = \beta\kappa_0^2\frac{\partial p^2}{\partial t}\right]$ term, and thus are described by a nonlinear wave equation in p."
In this example we have looked at a wave from a pulsating sphere, but the same result also hold for propagating plane waves and cylindrical waves [1]. In most of the situations considered in ultrasound, the condition $||x|| \gg \lambda$, that is, propagation lengths are much longer than wavelengths, is valid. Hence if one is interested only in the cumulative nonlinear effects, it is a fair assumption to leave the Lagrangian density out. For example, *Treeby et al.* neglect the Lagrangian density in their state-of-the-art acoustic simulation tool k-Wave [29]. In absence of $\mathcal{L}$, the nonlinear equations (2.15) and (2.17) read

$$\frac{\partial}{\partial t}\left(\kappa_0 p - \beta\kappa_0^2 p^2\right) = -\nabla\cdot v, \tag{2.33}$$

$$\rho_0\frac{\partial v}{\partial t} = -\nabla p, \tag{2.34}$$

and can be combined to give the second order lossless Westerwelt equation [15]:

$$\nabla^2 p - \frac{1}{c_0^2}\frac{\partial^2 p}{\partial t^2} = -\frac{\beta}{\rho_0 c_0^4}\frac{\partial^2 p^2}{\partial t^2} \tag{2.35}$$

A similar, but more involved derivation, yields the KZK-equation(Khokhlov-Zabolotskaya-Kuzentsov):

$$\frac{\partial^2 p}{\partial z \partial \tau} - \frac{c_0}{2}\nabla_\perp^2 p - \frac{\delta}{2c_0^3}\frac{\partial^3 p}{\partial \tau^3} = \frac{\beta}{2\rho_0 c_0^3}\frac{\partial^2 p^2}{\partial \tau^2} \tag{2.36}$$

The KZK-equation is used to model directional sound beams, propagating in the z-direction. The operator $\nabla_\perp^2 = \frac{\partial^2}{\partial x^2} + \frac{\partial^2}{\partial y^2}$ acts only perpendicular to the propagation direction, and δ is a factor that accounts for loss terms. This equation is widely used to model nonlinear waves in ultrasound [15, 18].

However, since local nonlinear effects might occur in wave-particle interaction, and we want an accurate description, we should not neglect the Lagrangian density.

A problem with the derivation of the continuity equation

In the case of a discontinuous density distribution, the Eulerian derivation of the continuity equation (2.1) in differential form is not valid. On deriving the equations, one starts with the assumption that the change of mass for an arbitrary control volume Ω_c must be equal to the flux of mass through the volume boundary $\partial\Omega_c$:

$$\frac{\mathrm{d}}{\mathrm{d}t}\int_{\Omega_c} \rho \mathrm{d}V = -\int_{\partial\Omega_c} v\rho \cdot n \mathrm{d}A \tag{2.37}$$

Then one applies the divergence theorem to get

$$\int_{\Omega_c} \frac{\partial \rho}{\partial t} + \nabla \cdot (\rho v) \mathrm{d}V = 0. \tag{2.38}$$

The statement of the divergence theorem for a smooth volume Ω reads [26]:

Let Ω and n the outward unit normal on $\partial\Omega$, and let $f(x,t)$ be a continuously differentiable vector function, i.e. $f \in C^1(\Omega)$. Then $\int_\Omega \nabla \cdot f \mathrm{d}V = \int_{\partial\Omega} f \cdot n \mathrm{d}A$.

But ρv is not always continuous, and hence the theorem cannot be used this way. One can do the derivation with test functions to get a weak formulation, but this is a different story [26, 24]. The differential form of the Euler equations require the ambient, or initial, distribution of mass, to be continuous. We will later see that the Lagrangian equivalent of (2.1) does not, and hence is more suited for our purpose.

The Eulerian form of the acoustic equations have many applications, but from the above investigations, it seems that the standard Eulerian equations for propagation of acoustic waves are not well suited for an accurate description of general wave-particle interaction.

Particles represented as a variation in material parameters

We have already seen some methods to include particles and heterogeneity in our model. A natural way of describing a particle in the material is through the material parameters. The particle is characterized by having different material properties than its surroundings. Material properties are represented in parameters that describe different aspects of a material, and materials have many different material properties: Electric conductivity, specific heat capacity, Young's modulus, etc. However, when we study acoustic waves, there are mainly two parameters of interest: The mass density ρ and the compressibility κ. They are defined as:

$$\rho = \frac{\mathrm{d}m}{\mathrm{d}V} \tag{2.39}$$

$$\kappa = -\frac{1}{V}\frac{\partial V}{\partial p} \tag{2.40}$$

As mentioned above, acoustic waves propagate as compression and expansion of the material, and how a material compresses and expand is mainly determined by its (mass) density and compressibility. At a particle these properties differ, often discontinuously, and this leads to changes in the wave propagation.

We define a particle to be a small, simply connected[6] region in the material, denoted Ω_p. For a single particle in $\mathbb{R}^3$, where the surrounding material and the particle have, respectively, constant material parameters ρ_m, κ_m,ρ_p and κ_p, we define

$$\rho_0(x,t) = \begin{cases} \rho_p & \text{for } x \in \Omega_p \\ \rho_m & \text{for } x \notin \Omega_p \end{cases} \qquad \kappa_0(x,t) = \begin{cases} \kappa_p & \text{for } x \in \Omega_p \\ \kappa_m & \text{for } x \notin \Omega_p. \end{cases} \tag{2.41}$$

Since the same equation describes the acoustic wave propagation both inside and outside the particle, we want to derive a wave equation that allows for inclusion of the material parameters in a natural way, without the ad hoc touch. As we will see, using a Lagrange formulation lets us do just that.

[6] Simply connected means that you can draw a curve between all points in the region without leaving it, and that it has no holes.

CHAPTER 3

Lagrangian formulation of the governing equations

In this chapter we introduce the Lagrangian description, and derive the governing equations formulated in Lagrangian coordinates. We also point at why these equations are better suited to model wave propagation in heterogeneous materials.

The Lagrangian description of a material (i.e. a fluid, solid, etc.) differs from the description we have used this far, the Eulerian description. In Eulerian coordinates, the governing equations are formulated to yield a value at fixed point in space at a given time. Thus, if for example one is interested in the velocity of a fluid, $v(x,t)$, the Eulerian description will give you the velocity of the fluid flowing past the spatial position x at time t. Since one does not usually care about the life of individual regions of a fluid, but rather the behavior of the fluid at given points (e.g. "will the pressure break the dam?"), this works very well. But if a pile of dry leaves were lying on the ground, and the wind started blowing, and you wanted to know how each single leave would be carried around by the wind, the Eulerian description would not be very good. It could give you information on the velocity of the particular leave drifting by, and possibly also the density of that leave, but it would be a cumbersome process to try and reconstruct each of the leaves' paths from this information. The Lagrangian description gives you an alternative. It describes the properties and movement of each point in you domain, uniquely determined from its starting position, its Lagrangian coordinate. The Lagrangian coordinates of the leaves would be their initial positions in the pile, and the solution to the Lagrangian equations of motion would give you each leaves' current velocity and position. We will see that the Lagrangian formulation leads to a much more convenient equation for conservation of mass, and incorporates heterogeneous material parameters in a natural way. It also solves the problem of the potentially moving particle, as we obtain equations for the motion of all points in material.

We now introduce the mathematical framework of the Lagrangian description, and derive the equations used to describe acoustic wave propagation in Lagrangian coordinates.

3.1. Mathematical formulation

Let $\mathbf{X} \in \Omega(0)$, with $\Omega(0) \subset \mathbb{R}^3$. We refer to $\Omega(0)$ as the reference, or initial, configuration.[1] Then the position of a point originally at situated the spatial position $\mathbf{X} = [X,Y,Z]^T$ at $t_0 = 0$ is given by $\mathbf{x} = [x,y,z]^T = \varphi(\mathbf{X},t)$, where φ is called the displacement function. Hence, its position at a given time t depends on its starting point $\mathbf{X}$, i.e. its Lagrangian coordinate. A natural requirement is that $\varphi(\mathbf{X},0) = \mathbf{X}$. Because of this it is common to define $\varphi(\mathbf{X},t) = \mathbf{X} + U(\mathbf{X},t)$,

[1] Boldface letters $\mathbf{X}$ and $\mathbf{x}$ are not used for vectors in general, but reserved for the coordinates of the reference and current configurations.

where $U(\mathbf{X},t)$ is the displacement from the starting point. Naturally, we require $U(\mathbf{X},0)=0$. The vector U is called the displacement vector. Written out we have

$$\varphi(\mathbf{X},t)=\mathbf{X}+U(\mathbf{X},t)=\begin{bmatrix}\varphi_i(\mathbf{X},t)\\ \varphi_j(\mathbf{X},t)\\ \varphi_k(\mathbf{X},t)\end{bmatrix}=\begin{bmatrix}X+U_i(\mathbf{X},t)\\ Y+U_j(\mathbf{X},t)\\ Z+U_k(\mathbf{X},t)\end{bmatrix}, \tag{3.1}$$

where the i,j,k subscripts signifies the x,y,z directions in Cartesian coordinates. We will refer to a region $\Omega(t)=\varphi(\Omega(0),t)$ as the deformed, or current, region. A graphical representation of the Lagrangian description can be seen in Figure 1. As we will see, the Lagrangian description

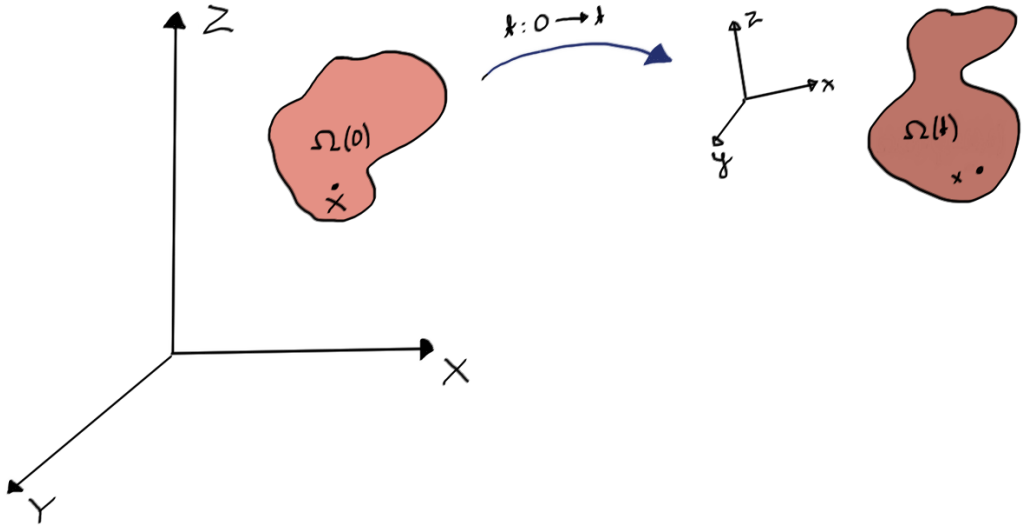

FIGURE 1. A control volume $\Omega(0)$ gets displaced in space, to $\Omega(t)=\varphi(\Omega(0),t)$. X,Y,Z are the Lagrangian coordinates, and x,y,z are the spatial/Eulerian coordinates.

offers two possible formulations of the equations of motion; either with respect to the reference configuration or with respect to the deformed configuration. The former is called the material description, and the latter is called the spatial decription. We will denote quantities evaluated in the reference position with capital letters, and quantities evaluated at the deformed configuration with lowercase letters. Hence, $F(\mathbf{X},t)=f(\varphi(\mathbf{X},t),t)$. The acceleration of a point is the temporal derivative of its velocity, and the difference in where one evaluates it is

$$\frac{\partial V(\mathbf{X},t)}{\partial t}=\frac{\partial V}{\partial t}+\nabla V\cdot\frac{\partial \mathbf{X}}{\partial t}=\frac{\partial V}{\partial t}, \tag{3.2}$$

since $\frac{\partial \mathbf{X}}{\partial t}=0$, and

$$\frac{\partial v(\varphi,t)}{\partial t}=\frac{\partial v}{\partial t}+\frac{\partial \varphi}{\partial t}\cdot\nabla_{\mathbf{x}}v=\frac{\partial v}{\partial t}+v\cdot\nabla_{\mathbf{x}}v. \tag{3.3}$$

Hence $\frac{\partial V(\mathbf{X},t)}{\partial t} = \frac{\partial v(\varphi,t)}{\partial t} + v(\varphi,t)\cdot\nabla_{\mathbf{x}} v(\varphi,t)$. The term $v\cdot\nabla_{\mathbf{x}} v$ is called the convective acceleration, and is also included in the total derivative $\frac{\mathrm{D}}{\mathrm{d}t}$ introduced in (2.6). The subscript $\mathbf{x}$ on the nabla operator indicates that the gradient is taken w.r.t. the deformed configuration $\mathbf{x}$.

φ as a mapping

Mathematically one can view the function φ as a mapping from some initial region to the current region; $\varphi : (\Omega(0),t) \to \Omega(t)$. The Lagrangian description is often used in continuum mechanics, a mathematical theory for modeling the behavior of matter as a collection of deformable bodies [22]. It is through this framework we will formulate our equations. A fundamental assumption in continuum mechanics is that matter occupies space completely and continuously. To quote *J.T. Oden* in [22]:
"Matter is not discrete; it is continuously distributed in one-to-one correspondence with points in some subset of $\mathbb{R}^3$*."*
The displacement function φ serves as this continuous, one-to-one correspondence between the reference configuration and the current configuration. Two important concepts in the description of displacement are the displacement gradient, the Jacobian of φ, and the Jacobian determinant. They are defined as

$$F(\mathbf{X},t) = \nabla\varphi(\mathbf{X},t) = \begin{bmatrix} \partial_X\varphi_i & \partial_Y\varphi_i & \partial_Z\varphi_i \\ \partial_X\varphi_j & \partial_Y\varphi_j & \partial_Z\varphi_j \\ \partial_X\varphi_k & \partial_Y\varphi_k & \partial_Z\varphi_k \end{bmatrix} = \begin{bmatrix} 1+\partial_X U_i & \partial_Y U_i & \partial_Z U_i \\ \partial_X U_j & 1+\partial_Y U_j & \partial_Z U_j \\ \partial_X U_k & \partial_Y U_k & 1+\partial_Z U_k \end{bmatrix}, \quad (3.4)$$

where we have used the notation $\frac{\partial}{\partial X} = \partial_X$ etc., and

$$J(\mathbf{X},t) = \det(F) \quad (3.5)$$

F and J becomes important in the Lagrangian formulation of both mass and momentum conservation.

3.2. Conservation of mass

Another fundamental assumption in continuum mechanics is that matter is neither destroyed or created during a deformation. This means that a region with an initial mass M_0 should still have mass M_0 at any later time, independent of its deformation, if no mass enter or leave it. On could think of a sloppy football; no matter how you squeeze it, it still weighs the same.

From this assumption we obtain the Lagrangian continuity equation. We define a region, or control volume, to be $B(t) = \{\varphi(\mathbf{X},t) : \varphi(\mathbf{X},0) \in B \subset \mathbb{R}^3\}$, i.e. $B(t)$ is a region of points initially located at B. Thus $B(0) = B$. We denote the mass density as $\rho(\mathbf{x},t)$, and $\rho(\mathbf{x},0) = \rho_0(\mathbf{X})$. We denote the mass of $B(t)$ as $M(t)$. The initial mass $M(0)$ is then given as

$$M(0) = \int_B \rho_0(\mathbf{X})\mathrm{d}V \quad (3.6)$$

where $\mathrm{d}V = \mathrm{d}X\mathrm{d}Y\mathrm{d}Z$, and should remain the same as $B(t)$ changes its position an configuration with time. That is,

$$M(0) = M(t) \quad \Longrightarrow \quad \int_B \rho_0(\mathbf{X})\mathrm{d}V = \int_{B(t)} \rho(\mathbf{x},t)\mathrm{d}v, \tag{3.7}$$

where $\mathrm{d}v = \mathrm{d}x\mathrm{d}y\mathrm{d}z$. We now take the volume integral over the deformed region back to the initial region to perform the integration over $B(0)$, and get [2]

$$\int_{B(t)} \rho(\mathbf{x},t)\mathrm{d}v = \int_B \rho(\mathbf{x},t)J\mathrm{d}V, \tag{3.8}$$

where J is the Jacobian determinant of the displacement, as introduced above.
The requirement that $M(0) = M(t)$ now reads

$$\int_B \rho_0(\mathbf{X})\mathrm{d}V = \int_B \rho(\mathbf{x},t)J\mathrm{d}V, \tag{3.9}$$

or

$$\int_B \rho_0(\mathbf{X}) - \rho(\mathbf{x},t)J\mathrm{d}V = 0. \tag{3.10}$$

Since B is arbritary, the integrand in (3.10) has to be zero for all t and $\mathbf{X}$. The continuity equation now takes the form

$$\rho(\mathbf{x},t) = \frac{\rho_0(\mathbf{X})}{J(\mathbf{X},t)}. \tag{3.11}$$

This is quite a different expression than its Eulerian equivalent (2.1). Once the deformation is known, we can simply compute the density $\rho(\mathbf{x},t)$ in the deformed material from the initial density $\rho_0(\mathbf{X})$ and the Jacobian determinant $J(\mathbf{X},t)$, and the computation does not involve taking spatial derivatives of the density. It is apparent that this formulation is more suited if one wants to include heterogeneous material parameters; the formulation allows ρ_0 to be discontinuous.

It is also interesting to note the following: The fundamental hypothesis of continuum mechanics says that there is a bijection between material and spatial coordinates. It can be shown that this requires for the Jacobian matrix to be invertible for all times [16]. This equivalent to $J(\mathbf{X},t) > 0, \quad \forall t \geq 0$ since the existence of F^{-1} implies $J(\mathbf{X},t) \neq 0$, and $J(\mathbf{X},0) = \det(F(\mathbf{X},0)) = \det(\mathrm{I}) = 1$,[2]. This condition also seem natural in the light of (3.10) since $J \leq 0$ would cause the density to blow up or become negative, which is clearly non-physical. The condition is sometimes referred to as the mathematical form of the assumption of impenetrability of matter [16].

[2] I is the 3×3 identity matrix.

3.3. Conservation of momentum

We continue to obtain the momentum equation in Lagrangian coordinates. The integral formulation of principle of conservation of momentum, in absence of body forces, is [22]

$$\frac{\mathrm{d}}{\mathrm{d}t}\int\limits_{B(t)} \rho(\mathbf{x},t)v(\mathbf{x},t)\mathrm{d}v = \int\limits_{\partial B(t)} \sigma(\mathbf{x},t)\mathrm{n}\mathrm{d}s. \tag{3.12}$$

Here $B(t)$ denotes the same kind of control volume as used in derivation of (3.11), and $\partial B(t)$ is the boundary[3] of $B(t)$. $\sigma(\mathbf{x},t)$ is known as the Cauchy stress tensor, and a detailed discussion on σ can be found in [22, 14]. σ is a 3×3 matrix that specifies the forces acting in a in a continuum. When we only hydrostatic pressure, the stress tensor reduces to $\sigma = -p(\mathbf{x},t)\mathrm{I}$, where I is the 3×3 identity matrix [16]. n is the outward unit normal vector in the deformed volume and ds is the surface differential of $\partial B(t)$. We now want to relate the surface integrals over the deformed and initial control volume.

Nanson's formula

Nanson's formula relates the normal differentials n$\mathrm{d}s$ and N$\mathrm{d}S$ on $\partial B(t)$ and ∂B. We have the following relation between the normal differentials and the volume differentials:

$$\mathrm{d}\mathbf{X}\cdot\mathrm{N}\mathrm{d}S = \mathrm{d}V \qquad \text{and} \qquad \mathrm{d}\mathbf{x}\cdot\mathrm{n}\mathrm{d}s = \mathrm{d}v. \tag{3.13}$$

Taking the total differential d$\mathbf{x}$ w.r.t. $\mathbf{X}$ gives

$$\mathrm{d}\mathbf{x} = \begin{bmatrix}\mathrm{d}x\\ \mathrm{d}y\\ \mathrm{d}z\end{bmatrix} = \begin{bmatrix}\partial_X x & \partial_Y x & \partial_Z x\\ \partial_X y & \partial_Y y & \partial_Z y\\ \partial_X z & \partial_Y z & \partial_Z z\end{bmatrix}\begin{bmatrix}\mathrm{d}X\\ \mathrm{d}Y\\ \mathrm{d}Z\end{bmatrix}, \tag{3.14}$$

or in terms of the displacement gradient F,

$$\mathrm{d}\mathbf{x} = F\mathrm{d}\mathbf{X}. \tag{3.15}$$

From the change-of-variable formula for volume integration we know that the volume differentials are related by $\mathrm{d}v = J\mathrm{d}V$. Hence,

$$J\mathrm{d}\mathbf{X}\cdot\mathrm{N}\mathrm{d}S = \mathrm{d}\mathbf{x}\cdot\mathrm{n}\mathrm{d}s \quad\Longrightarrow\quad \mathrm{d}\mathbf{X}\cdot J\mathrm{N}\mathrm{d}S = F\mathrm{d}\mathbf{X}\cdot\mathrm{n}\mathrm{d}s = \mathrm{d}\mathbf{X}\cdot F^T\mathrm{n}\mathrm{d}s, \tag{3.16}$$

and since F is assumed invertible, we obtain Nanson's formula

$$JF^{-T}\mathrm{N}\mathrm{d}S = \mathrm{n}\mathrm{d}s \tag{3.17}$$

where $F^{-T} = (F^{-1})^T$.

[3] We require $\partial B(t)$ to be piecewise continuous.

The Lagrangian momentum equation

We are now in a position to do the integration of (3.12) over the reference configuration. Using (3.17) we have

$$\int_{\partial B(t)} \sigma(\mathbf{x},t)\mathrm{n}\mathrm{d}s = \int_{\partial B} J\sigma(\mathbf{x},t)F^{-T}\mathrm{N}\mathrm{d}S. \tag{3.18}$$

This transition is known as the Piola transform [22]. The transformed volume integral from (2.6) is

$$\int_{B(t)} \rho(\mathbf{x},t)v(\mathbf{x},t)\mathrm{d}v = \int_{B} \rho(\mathbf{x},t)V(\mathbf{X},t)J\mathrm{d}V = \int_{B} \rho_0(\mathbf{X})V(\mathbf{X},t)\mathrm{d}V, \tag{3.19}$$

since, from (3.11), $\rho_0 = J\rho$. The integral formulation of the conservation of momentum in the reference configuration thus becomes

$$\frac{\mathrm{d}}{\mathrm{d}t}\int_{B} \rho_0(\mathbf{X})V(\mathbf{X},t)\mathrm{d}V = \int_{\partial B} J\sigma(\mathbf{x},t)F^{-T}\mathrm{N}\mathrm{d}S. \tag{3.20}$$

The expression $P = J\sigma F^{-T}$ appearing in the surface integral is known as the Piola-Kirchhoff stress tensor, and relates stress in a deformed configuration to the stress in the reference configuration [22]. Using the tensor form of the divergence theorem [22], where ∇ denotes the divergence w.r.t. the Lagrangian coordinates, and pulling the time derivative inside the volume integral, we get

$$\int_{B} \rho_0\frac{\partial V}{\partial t}\mathrm{d}V = \int_{B} \nabla\cdot P\mathrm{d}V \quad \Longrightarrow \quad \int_{B} \rho_0\frac{\partial V}{\partial t} - \nabla\cdot P\mathrm{d}V = 0. \tag{3.21}$$

Again, since B is arbitrary, the integrand has to be zero for any control volume. Hence, the differential form of conservation of momentum in Lagrangian coordinates is:

$$\rho_0\frac{\partial V}{\partial t} = \nabla\cdot P \tag{3.22}$$

This equation looks both unpleasant and simple. Compared to its Eulerian equivalent, we see that we don't have a Lagrangian density $\mathcal{L}(x,t)$, which is nice. Another nice property is that we don't require spatial gradients of the density; nowhere in the derivation of neither (3.11) or (3.22) do we make the assumption that ρ or ρ_0 is continuous in space. But we have gained some complexity by introducing the Piola-Kirchhoff tensor. At first glance it is not very clear how one should handle $\nabla\cdot P = \nabla\cdot J\sigma F^{-T}$, neither analytically or numerically, but the following will make it more clear.

The Piola-Kirchhoff stress tensor

The Piola-Kirchhoff stress tensor relates the pressure in the deformed configuration to the forces in the reference configuration. To analyze P, we start by looking at JF^{-T}. A result from linear algebra simplifies things:

Let A be a invertible, square matrix in $\mathbb{R}^{n\times n}$. Let C_A be the cofactor matrix of A. Then

$$A^{-1} = \frac{1}{\det(A)}(C_A)^T, \tag{3.23}$$

where C_A of A is defined as

$$C_A = \begin{pmatrix} c_{11} & c_{12} & \dots & c_{1n} \\ c_{21} & c_{22} & \dots & c_{2n} \\ \vdots & \vdots & \ddots & \vdots \\ c_{n1} & c_{n2} & \dots & c_{nn} \end{pmatrix}, \tag{3.24}$$

and the cofactors are $c_{i,j} = (-1)^{i+j}\det(M_{i,j})$, and M_{ij} is the ij'th minor of A. The minor M_{ij} of A is the matrix A with row i and column j removed. For $A \in R^{3\times 3}$, the minor M_{21} would be

$$M_{21} = \begin{pmatrix} a_{12} & a_{13} \\ a_{32} & a_{33} \end{pmatrix}. \tag{3.25}$$

Since F is a square, invertible matrix, we have $JF^{-T} = C_F$. Calculation of C_F in 2 dimensions give

$$C_F = \begin{bmatrix} 1+\partial_Y U_j & -\partial_X U_j \\ -\partial_Y U_i & 1+\partial_X U_i \end{bmatrix}. \tag{3.26}$$

Now we show that $\nabla \cdot C_F = 0$. The divergence of the tensor C_F is

$$\nabla \cdot C_F = \nabla \cdot \begin{bmatrix} c_{11} & c_{12} & c_{13} \\ c_{21} & c_{22} & c_{23} \\ c_{31} & c_{32} & c_{33} \end{bmatrix} = \begin{bmatrix} \partial_X c_{11} + \partial_Y c_{12} + \partial_Z c_{13} \\ \partial_X c_{21} + \partial_Y c_{22} + \partial_Z c_{23} \\ \partial_X c_{31} + \partial_Y c_{32} + \partial_Z c_{33} \end{bmatrix}. \tag{3.27}$$

Writing the cofactors of the first component in terms of $\varphi(\mathbf{X},t) = [\varphi_i, \varphi_j, \varphi_k]^T$ we get

$$\begin{aligned} c_{11} &= \partial_Y \varphi_j \partial_Z \varphi_k - \partial_Z \varphi_j \partial_Y \varphi_k \\ c_{12} &= -(\partial_X \varphi_j \partial_Z \varphi_k - \partial_Z \varphi_j \partial_X \varphi_k) \\ c_{13} &= \partial_X \varphi_j \partial_Y \varphi_k - \partial_Z \varphi_j \partial_Y \varphi_k. \end{aligned}$$

The first row in $\nabla \cdot C_F$ equals $\nabla \cdot [c_{11}, c_{12}, c_{13}]$, and direct calculation gives

$$\begin{aligned} \nabla \cdot [c_{11}, c_{12}, c_{13}] = {} & \partial_X \partial_Y \varphi_j \partial_Z \varphi_k + \partial_Y \varphi_j \partial_X \partial_Z \varphi_k - \partial_X \partial_Z \varphi_j \partial_Y \varphi_k - \partial_Z \varphi_j \partial_X \partial_Y \varphi_k \\ & - \partial_Y \partial_X \varphi_j \partial_Z \varphi_k - \partial_X \varphi_j \partial_Y \partial_Z \varphi_k + \partial_Y \partial_Z \varphi_j \partial_X \varphi_k + \partial_Z \varphi_j \partial_Y \partial_X \varphi_k \\ & + \partial_Z \partial_X \varphi_j \partial_Y \varphi_k + \partial_X \varphi_j \partial_Z \partial_Y \varphi_k - \partial_Z \partial_Y \varphi_j \partial_X \varphi_k - \partial_Y \varphi_j \partial_Z \partial_X \varphi_k = 0. \end{aligned}$$

The same holds for the j and k component of $\nabla \cdot C_F$. Remembering that $\sigma(\mathbf{x},t) = -p(\mathbf{x},t)\mathrm{I}$, we have that $P = \sigma C_F = -pC_F$. The divergence of a scalar-matrix product is

$$\nabla \cdot (pC_F) = (C_F)^T \nabla p + p(\nabla \cdot C_F), \tag{3.28}$$

so from what we have just shown,

$$\rho_0 \frac{\partial V}{\partial t} = -C_F^T \nabla p. \tag{3.29}$$

Written out in component form, in two dimensions, with $V = [V_i, V_j]^T$, the equation for conservation of momentum reads

$$\rho_0 \frac{\partial}{\partial t} \begin{bmatrix} V_i \\ V_j \end{bmatrix} = - \begin{bmatrix} 1 + \partial_Y U_j & -\partial_Y U_i \\ -\partial_X U_j & 1 + \partial_X U_i \end{bmatrix} \begin{bmatrix} \partial_X p \\ \partial_Y p \end{bmatrix}. \tag{3.30}$$

3.4. An evolution equation for the pressure

Obtaining a valid partial differential equation for the pressure is not as straight forward as one would think, given (3.11). Not much literature on the topic exists, but it seems it is common to do certain assumptions on the acoustic quantities. We now discuss these assumptions and follow the derivation of a pressure evolution equation by *B. A. Angelsen* in [4].

The acoustic assumption

The acoustic assumption concerns the size of certain acoustic quantities. It is common to say that the theory of acoustics is an infinitesimal theory, meaning that e.g. the acoustic pressure and density, defined as the deviation from their static values, are very small quantities. Following the introductory discussion in *R. T. Beyer*'s book *Nonlinear Acoustics* [6], we introduce the acoustic Mach number, M. M is defined as the ratio of maximum particle velocity v_0 over local sound velocity c_0, and we require $M = \frac{v_0}{c_0} \ll 1$. We don't present the argument, but this leads to a condition on the spatial derivative on the displacement U:

$$\max\left(\frac{\partial U}{\partial x}\right) = \mathcal{O}(M) \tag{3.31}$$

From a similar derivation to the one in section 3.3, the 1-D version of the second order wave equation can be shown to be [6]

$$\frac{\partial^2 U}{\partial t^2} = \frac{c_0^2}{\left(1 + \frac{\partial U}{\partial x}\right)^2} \frac{\partial^2 U}{\partial x^2}, \tag{3.32}$$

and the acoustic assumption serves as a justification for linearization, since $\left(1 + \frac{\partial U}{\partial x}\right)^2 \leq (1 + M)^2 \approx 1$. Since the linear wave equation in Eulerian coordinates is

$$\frac{\partial^2 U}{\partial t^2} = c_0^2 \frac{\partial^2 U}{\partial x^2}, \tag{3.33}$$

the linear wave equation in Lagrangian and Eulerian coordinates coincides, and this also serves as a justification of the linearization of the Eulerian equations. It can also be shown that this leads to similar linear Lagrangian and Eulerian equations for higher dimensions, by assuming $C_F \approx I$ [30].

Angelsen's equation

The derivation starts by showing that one can assume $|\nabla \cdot U| \leq M$. The Jacobian determinant J is approximated to first order in ∂U as

$$J \approx 1 + \frac{\partial U_i}{\partial X} + \frac{\partial U_j}{\partial Y} + \frac{\partial U_k}{\partial Z} = 1 + \nabla \cdot U. \tag{3.34}$$

The condensation, or relative change in density, is defined as $\frac{\rho'}{\rho_0}$, and from (3.11) we get

$$\frac{\rho'}{\rho_0} = \frac{\rho_0 \left(\frac{1}{J} - 1\right)}{\rho_0} = \frac{1}{J} - 1 \approx \frac{1}{1 + \nabla \cdot U} - 1. \tag{3.35}$$

A second order Taylor expansion of this expression gives

$$\frac{\rho'}{\rho_0} \approx 1 + \nabla \cdot U + (\nabla \cdot U)^2 - 1 = \nabla \cdot U + (\nabla \cdot U)^2, \tag{3.36}$$

justified by $|\nabla \cdot U| \leq M \ll 1$. In terms of the condensation, the nonlinear equation of state is [15]

$$p = A\left(\frac{\rho - \rho_0}{\rho_0}\right) + \frac{B}{2}\left(\frac{\rho - \rho_0}{\rho_0}\right)^2 \tag{3.37}$$

Substituting the expression from (3.36) in to (3.37), discarding terms of order three or higher, yields the relation

$$p = A\left(\frac{\rho'}{\rho_0}\right) + \frac{B}{2}\left(\frac{\rho'}{\rho_0}\right)^2 \approx -A\nabla \cdot U + A\beta\left(\nabla \cdot U\right)^2, \tag{3.38}$$

where again $\beta = 1 + \frac{B}{2A}$. We now want to invert this relation. Solving for $\zeta = \nabla \cdot U$ and $k = \frac{p}{A}$, we get

$$\beta\zeta^2 - \zeta - k = 0 \quad \Longrightarrow 2\beta\zeta = 1 \pm \sqrt{1 + 4\beta k}. \tag{3.39}$$

We choose the negative root, since the other choice would leave us with $\nabla \cdot U = \frac{1}{2\beta}$ when $p = 0$. Since $k = \frac{p}{A} \ll 1$, we can approximate the root with its Taylor series up to second order [4], to get

$$\zeta \approx \frac{1}{2\beta}\left(1 - \left(1 + \frac{1}{2}4\beta k - \frac{1}{8}(4\beta k)^2\right)\right) = \left(-k + \beta k^2\right). \tag{3.40}$$

Hence, using that $\kappa_0 = \frac{1}{\rho_0 c_0^2} = \frac{1}{A}$ we get

$$\kappa_0 p - \beta(\kappa_0 p)^2 = -\nabla \cdot U \quad \text{or} \quad K(p) = -\nabla \cdot U \quad \text{where} \quad K(p) = \kappa_0 p - \beta(\kappa p)^2 \tag{3.41}$$

To get the equation presented in [3], one proceeds to take the material derivative of (3.41), to get

$$K'(p)\frac{\partial p}{\partial t} = -\nabla \cdot V, \tag{3.42}$$

where $K'(p) = \kappa_0 - 2\beta\kappa_0^2 p$ is known as the nonlinear elastic volume compressibility [4, 17]. There are certain similarities between this equation and the nonlinear pressure equation in Eulerian coordinates,

$$\frac{\partial}{\partial t}\left(\kappa_0 p - \beta\kappa_0^2 p^2\right) = K'(p)\frac{\partial p}{\partial t} = -\nabla \cdot v + \kappa_0 \frac{\partial}{\partial t}\mathcal{L}(x,t). \tag{3.43}$$

Again, we have lost the Lagrangian density $\mathcal{L}(\mathbf{x},t)$, but it required an additional assumption. The approximations that led to (3.42) are justified by the acoustic assumption, and by keeping

first order terms, instead of linearizing completely as in (3.32), but it is unclear what consequences these approximations have on the accuracy of the equation. In the paper describing the acoustic simulation tool Abersim [30], the authors use a Lagrangian description and equation (3.42) (where they include a loss term), and approximate the Piola-Kirchhoff tensor in (3.22) as $\nabla \cdot P \approx \nabla p$. Comparing with the Eulerian equations, we see that this is equivalent to solving the system (2.33)-(2.34).

A different approach

Since the density is given directly once we know the deformation, as in (3.11), we can, in principle, obtain the pressure directly. In terms of the condensation $\frac{\rho'}{\rho_0} = \frac{1}{J} - 1$ and the linear and nonlinear equation of state, we have that

$$p = \frac{1}{\kappa_0}\left(\frac{1}{J} - 1\right) \quad \text{or} \quad p = \frac{1}{\kappa_0}\left(\frac{1}{J} - 1\right) + \frac{B}{2}\left(\frac{1}{J} - 1\right)^2. \tag{3.44}$$

For analytical purposes and for comparison with the Eulerian equations we also derive the differential form of (3.44). For that we need a result on the derivative of J. From [16] we have the result that for a continuously differentiable invertible matrix $M(t)$

$$\frac{\partial}{\partial t}\det(M) = \det(M)\mathrm{tr}\left(M^{-1}\frac{\partial}{\partial t}M\right), \tag{3.45}$$

where, for a square matrix $A \in \mathbb{R}^{m\times m}$, the trace is $\mathrm{tr}(A) = \sum_{i=1}^{m} a_{ii}$. In the case of the deformation gradient F, we have

$$\frac{\partial}{\partial t}F = \frac{\partial}{\partial t}\nabla\varphi(\mathbf{X},t) = \nabla\frac{\partial}{\partial t}\varphi(\mathbf{X},t) = \nabla V(\mathbf{X},t). \tag{3.46}$$

We now need a relation between the gradient w.r.t. the reference configuration and the gradient w.r.t. the deformed configuration. Since $v(\mathbf{x},t) = V(\mathbf{X},t)$, the chain rule gives, for component i,

$$\frac{\partial V_i}{\partial X} = \frac{\partial v_i}{\partial x}\frac{\partial x}{\partial X} + \frac{\partial v_i}{\partial y}\frac{\partial y}{\partial X} + \frac{\partial v_i}{\partial z}\frac{\partial z}{\partial X}. \tag{3.47}$$

Carrying out the computation for all the components in $\nabla_{\mathbf{x}} v$, one finds that the gradients are related by the deformation gradient F as

$$\nabla V = \nabla_{\mathbf{x}} v F \quad \text{or} \quad \nabla_{\mathbf{x}} v = \nabla V F^{-1}. \tag{3.48}$$

Going back to (3.45), with $J = \det(F)$, we have

$$\frac{\partial}{\partial t}J = J\mathrm{tr}\left(F^{-1}\frac{\partial}{\partial t}F\right) = J\mathrm{tr}\left(F^{-1}\nabla V\right) = J\mathrm{tr}\left(\nabla V F^{-1}\right) = J\mathrm{tr}\left(\nabla_{\mathbf{x}} v\right) = J\nabla_{\mathbf{x}}\cdot v, \tag{3.49}$$

since $\mathrm{tr}\,(AB) = \mathrm{tr}\,(BA)$ for matrices $A, B \in \mathbb{R}^{m\times m}$, and $\mathrm{tr}\,(\nabla_{\mathbf{x}} v) = \nabla_{\mathbf{x}}\cdot v$.

If we now take the material derivative of the pressure equation (3.44) obtained from the linear equation of state, we get

$$\frac{\partial p}{\partial t} + \nabla_{\mathbf{x}} p \cdot v = -\frac{1}{\kappa_0}\frac{\nabla_{\mathbf{x}}\cdot v}{J}. \tag{3.50}$$

We note that a linearization according to the acoustic assumption that $J \approx 1$, leads to a equation similar to the linear Eulerian pressure equation (2.5), i.e.

$$\frac{\partial p}{\partial t} = -\frac{1}{\kappa_0} \nabla_{\mathbf{x}} \cdot v. \tag{3.51}$$

We can also express (3.50) in the reference configuration, using that[4] $\nabla_{\mathbf{x}} \cdot v = \frac{1}{J} \nabla \cdot \left(J F^{-T} V \right)$:

$$\frac{\partial p}{\partial t} = -\frac{1}{\kappa_0 J^2} \nabla \cdot \left(J F^{-1} V \right) \tag{3.52}$$

A derivation with the nonlinear equation of state yields

$$\frac{\partial p}{\partial t} + \nabla_{\mathbf{x}} p \cdot v = -\frac{1}{\kappa_0} (1 - B) \frac{\nabla_{\mathbf{x}} \cdot v}{J} - B \frac{\nabla_{\mathbf{x}} \cdot v}{J^2}. \tag{3.53}$$

These equations are an alternative to the pressure equation (3.42). As there is, to our knowledge, no literature describing this latter approach or equations (3.50), (3.52) and (3.53), we will not pursue it further.

Summing up, the Lagrangian equations describing acoustic wave propagation are

$$K'(p) \frac{\partial p}{\partial t} = -\nabla \cdot V \tag{3.54}$$

$$\rho_0 \frac{\partial V}{\partial t} = -\nabla \cdot P, \tag{3.55}$$

or written out in two dimensions,

$$K'(p) \frac{\partial p}{\partial t} = -\frac{\partial V_i}{\partial X} - \frac{\partial V_j}{\partial Y} \tag{3.56}$$

$$\rho_0 \frac{\partial}{\partial t} \begin{bmatrix} V_i \\ V_j \end{bmatrix} = - \begin{bmatrix} 1 + \partial_Y U_j & -\partial_Y U_i \\ -\partial_X U_j & 1 + \partial_X U_i \end{bmatrix} \begin{bmatrix} \partial_X p \\ \partial_Y p \end{bmatrix}. \tag{3.57}$$

The equations must be equipped with suitable initial and boundary conditions. We will return to this in Chapter 5, when we construct a numerical method to for solving them.

[4] This relation is obtained by similar arguments to those yielding (3.29).

CHAPTER 4

Energy, viscoelasticity and attenuation

In this section we look at a property that is essential to equations derived from conservations laws; a feature known as conservation of energy. We then introduce the concept of viscoelasticity, to account for attenuation, i.e. loss of energy, in our equations.

4.1. Conservation of Energy

Physically, acoustic waves can be interpreted as the interaction of the potential and kinetic energy of the particles in the material in which the wave propagates. The propagation appears as compression and expansion of the material. When the material is compressed, the wave energy exists as potential energy, and during the expansion this energy is converted into kinetic energy. Hence, one can say that kinetic energy depends on the motion of the material, while potential energy depends on the deformation. The principle of conservation of energy[1] says that the sum of potential and kinetic energy is constant in absence of sources. It is useful for proving uniqueness of solutions and stability of numerical schemes, and also for calculating acoustic intensity [28].

It is natural to write the total energy density as a sum of the kinetic and potential energy density:

$$\varepsilon_T = \varepsilon_K + \varepsilon_P \tag{4.1}$$

The kinetic energy density is generally defined to be $\varepsilon_K = \frac{1}{2}\rho v^2$, or $\varepsilon_K = \frac{1}{2}\rho_0 v^2$, for the Eulerian equations [6]. As we pointed out earlier, there seems to some disagreement on what the potential energy density is [28]. We now present a quite general approach to find expression for ε_P using thermodynamics.

Let $\mathcal{U}$ be the internal energy[2] of a material. Then the first law of thermodynamics states that

$$\mathrm{d}\mathcal{U} = \delta Q + \delta W. \tag{4.2}$$

Equation (4.2) says that the change in internal energy ($\mathrm{d}\mathcal{U}$) is equal to the heat transfer into the system (δQ) plus the work done on the system (δW) [28]. The δ's are known as inexact differentials, and will soon be replaced by exact ones. At this point we assume that the compression/expansion process is adiabatic, i.e. that there is no heat transfer during the process. Then $\delta Q = 0$. This is a common assumption in acoustics, and is motivated by assuming that pressure variations are so rapid that there is no time for heat flow [9]. For an ideal fluid we have $\delta W = -p\mathrm{d}V$, and from conservation of mass we have $\rho V = m$. To get the potential energy

[1] energy=acoustic energy.

[2] Internal energy is the total energy of a system excluding kinetic energy and potential energy due to external forces, i.e. gravity.

per mass, we first set $m = 1$, and get that $\mathrm{d}V = -\frac{\mathrm{d}\rho}{\rho^2}$. Inserting this in the linear compressibility relation (2.40) we get

$$\kappa_0 = -\frac{1}{V}\frac{\partial V}{\partial p} = \rho\frac{1}{\rho^2}\frac{\mathrm{d}\rho}{\mathrm{d}p} \quad \Longrightarrow \quad \mathrm{d}\rho = \kappa_0\rho\mathrm{d}p \quad \Longrightarrow \quad \mathrm{d}U = \kappa_0\frac{p}{\rho}\mathrm{d}p \tag{4.3}$$

The internal energy (per mass) and the potential energy density then relates as $\rho\mathrm{d}\mathcal{U} = \mathrm{d}\varepsilon_P$ [6]. Integrating $\mathrm{d}\varepsilon_P$ from 0 to p, we get that the potential energy density relative to the undisturbed state is

$$\varepsilon_P = \kappa_0 \int_0^p q\mathrm{d}q = \frac{1}{2}\kappa_0 p^2 \tag{4.4}$$

This is the most common expression for ε_P, found in e.g. [4, 28, 6]. Before we continue, we look closer at energy conservation.

Acoustic intensity and Power

To see how energy is conserved in the acoustic equations, we look at the closely related concepts acoustic intensity and power. Acoustic intensity is defined as $\mathcal{I}(\mathbf{x}, t) = pv$, and represents the instantaneous energy flow per unit area [8]. The power $\mathcal{P}(\mathbf{x}, t)$ of a volume $\Omega(t)$ is the work per unit time from the forces acting on $\Omega(t)$, and can, in absence of body forces, be written in terms of the acoustic intensity [22]:

$$\mathcal{P}(\mathbf{x}, t) = -\int_{\partial\Omega(t)} p(v \cdot n)\mathrm{d}s = -\int_{\partial\Omega(t)} \mathcal{I} \cdot n\mathrm{d}s \tag{4.5}$$

One can then show that the total acoustic energy $\mathcal{E}(t)$ of Ω, given as

$$\mathcal{E}(t) = \int_{\Omega(t)} \varepsilon_T \mathrm{d}v, \tag{4.6}$$

and the power is related as

$$\frac{\mathrm{d}}{\mathrm{d}t}\mathcal{E} = \mathcal{P} + Q, \tag{4.7}$$

where Q represents heat sources, which we assume to be zero [22]. In fact this is a more specific version of the first law of thermodynamics given in equation (4.2). Hence it becomes clear that the energy of a wave is conserved in some domain $\Omega(t)$, if p or v (or both) are zero at the entire boundary $\partial\Omega$, since this yields

$$\frac{\mathrm{d}}{\mathrm{d}t}\mathcal{E} = \mathcal{P} = -\int_{\partial\Omega(t)} p(v \cdot n)\mathrm{d}s = 0. \tag{4.8}$$

From (4.7) we can also obtain a energy-intensity equation. In integral form we have

$$\frac{\mathrm{d}}{\mathrm{d}t}\int_{\Omega(t)} \varepsilon_T \mathrm{d}v = -\int_{\partial\Omega(t)} \mathcal{I} \cdot n\mathrm{d}s = -\int_{\Omega(t)} \nabla_{\mathbf{x}} \cdot \mathcal{I}\mathrm{d}v \implies \int_{\Omega(t)} \frac{\partial \varepsilon_T}{\partial t} + \nabla_{\mathbf{x}} \cdot \mathcal{I}\mathrm{d}v = 0, \tag{4.9}$$

and since $\Omega(t)$ is arbitrary we have

$$\frac{\partial \varepsilon_T}{\partial t} + \nabla_{\mathbf{x}} \cdot \mathcal{I} = 0 \tag{4.10}$$

We will now see that we have energy conservation for the linear Eulerian equations, when

$$\mathcal{E}(t) = \int_\Omega \frac{1}{2}\rho_0 v^2 + \frac{1}{2}\kappa_0 p^2 \mathrm{d}V. \tag{4.11}$$

We want to show that $\frac{\partial \mathcal{E}(t)}{\partial t} = 0$, and we get

$$\frac{\mathrm{d}\mathcal{E}(t)}{\mathrm{d}t} = \frac{\mathrm{d}}{\mathrm{d}t}\int_\Omega \frac{1}{2}\rho_0 v^2 + \frac{1}{2}\kappa_0 p^2 \mathrm{d}V = \int_\Omega \rho_0 v \cdot \frac{\partial v}{\partial t} + \kappa_0 p \frac{\partial p}{\partial t}\mathrm{d}V. \tag{4.12}$$

Substituting from the linear equations (2.4) and (2.6) and integrating by parts we get

$$\frac{\mathrm{d}\mathcal{E}(t)}{\mathrm{d}t} = \int_\Omega -v \cdot \nabla p - p\nabla \cdot v \mathrm{d}V = \int_\Omega p\nabla \cdot v - p\nabla \cdot v \mathrm{d}V = 0. \tag{4.13}$$

We continue to find an expression for ε_P in the nonlinear case: κ_0 is the linear compressibility, and it can be shown that a nonlinear compressibility relation is [4, 17]

$$K'(p) = -\frac{1}{V}\frac{\partial V}{\partial p}, \qquad \text{where} \qquad K'(p) = \kappa_0 - 2\beta\kappa_0^2 p. \tag{4.14}$$

Hence the potential energy density for nonlinear waves is found to be

$$\varepsilon_P^{nl} = \int_0^p qK'(q)\mathrm{d}q = \frac{1}{2}\kappa_0 p^2 - \frac{2}{3}\beta\kappa_0^2 p^3. \tag{4.15}$$

We note that for nonlinear waves, the Lagrangian density that appears in (2.15) and (2.17), $\mathcal{L}(x,t) = \frac{1}{2}\rho v^2 - \frac{1}{2}\kappa_0 p^2$, is not really the Lagrangian density, since $\mathcal{L}(x,t) \neq \varepsilon_K - \varepsilon_P^{nl}$.
We now show that the nonlinear Eulerian equations, when $\mathcal{L}$ is neglected, also obey the principle of conservation of energy when ε_P^{nl} is the potential energy density. The nonlinear wave equations are

$$K'(p)\frac{\partial p}{\partial t} = -\nabla \cdot v + \kappa_0 \frac{\partial}{\partial t}\mathcal{L}(x,t) \tag{4.16}$$

$$\rho_0 \frac{\partial v}{\partial t} = -\nabla p - \nabla \mathcal{L}(x,t). \tag{4.17}$$

Ignoring the terms involving $\mathcal{L}$, we get

$$\begin{aligned}\frac{\mathrm{d}\mathcal{E}(t)}{\mathrm{d}t} &= \frac{\mathrm{d}}{\mathrm{d}t}\int_\Omega \frac{1}{2}\rho_0 v^2 + \frac{1}{2}\kappa_0 p^2 - \frac{2}{3}\beta\kappa_0^2 p^3 \mathrm{d}V \\ &= \int_\Omega \rho_0 v \cdot \frac{\partial v}{\partial t} + p(\kappa_0 - 2\beta\kappa_0^2 p)\frac{\partial p}{\partial t}\mathrm{d}V \\ &= \int_\Omega \rho_0 v \cdot \frac{\partial v}{\partial t} + pK'(p)\frac{\partial p}{\partial t}\mathrm{d}V\end{aligned}$$

Substitution of (4.16) (4.17) and integration by parts then yields

$$\frac{\mathrm{d}\mathcal{E}(t)}{\mathrm{d}t} = \int_\Omega -v\cdot\nabla p - p\nabla\cdot v \mathrm{d}V = \int_\Omega p\nabla\cdot v - p\nabla\cdot v \mathrm{d}V = 0, \tag{4.18}$$

as it should. However, if include $\mathcal{L}$ in the calculation, things do not work out so smoothly: Carrying out the same calculation, we are left with

$$\frac{\mathrm{d}\mathcal{E}(t)}{\mathrm{d}t} = \int_\Omega \kappa_0 p\frac{\partial}{\partial t}\mathcal{L} - v\cdot\nabla\mathcal{L}\mathrm{d}V = \int_\Omega \nabla\cdot v\left(\frac{1}{2}\rho_0 v^2 + \kappa_0 p^2\right)\mathrm{d}V. \tag{4.19}$$

Since all the terms in the parenthesis are positive, we can rewrite this as

$$\left|\frac{\mathrm{d}\mathcal{E}(t)}{\mathrm{d}t}\right| \leq \int_\Omega |\nabla\cdot v| C\mathrm{d}V, \tag{4.20}$$

where $C>0$ is some constant, and it is clear that for $\mathcal{E}$ to be constant, we have to have $\nabla\cdot v = 0$ in all of Ω, i.e. no wave.

Energy conservation for the Lagranigan equations

As we saw in (4.20), we did not get the wanted energy conservation when we included the Lagrangian density term the Eulerian equations. Attempting to show energy conservation for equation (3.29), (3.42) and (3.52), using both the nonlinear potential energy expressions, also fails. Hence the problem can lie either in the formulation of the potential energy ε_P or equations (3.42) and (3.52), or it can be related to the equation of state. In the, sometimes impervious, literature of continuum mechanics and elasticity, e.g. [22, 19], and also in [15], the potential energy density is sometimes referred to as the strain energy density. The strain energy density is a functional on the form

$$S = S(I_1, I_2, I_3) \quad \text{where} \quad \lambda_i = \mathrm{eig}(F^T F) \quad \text{and} \quad I_n = I_n(\lambda_i) \quad i,n = 1,2,3. \tag{4.21}$$

Here $\mathrm{eig}(A)$ denotes the eigenvalues of the matrix A. According to [22], if the correct strain energy density function is known, the stress(in an elastic) material can be derived from S. Attempts to show this, and energy conservation, with the Lagrangian equations did not succeed.

A motivation for the investigation of conservation of energy has been that it could serve as a verification device for the Lagrangian equations, but this has not been successful. As a last note on conservation of energy, we can say that it seems that the standard expression $\frac{1}{2}\kappa_0 p^2$ is a fair approximation to the potential energy density. When we calculate the total energy in simulations using (4.11), energy conservation seem to hold.

4.2. Viscoelasticity and attenuation

To include the effects of attenuation in our model we consider viscoelastic effects. Attenuation, or loss of energy, in acoustic waves is due to microscopic phenomena, where the kinetic and potential energy of the molecules are transferred to other degrees of freedom, e.g. vibrational or rotational energy, or changes in the molecular configuration [14, 4]. Then the assumption that the process is adiabatic, which we utilized in deriving the potential energy in (4.4) and (4.15), is no longer valid. When a material is compressed, it might not expand to its initial state

afterwards, and some of the (vibrational) energy is lost. A fully elastic material is a material where no energy is lost due to this kind of behaviour, and a fully viscous material is a material where all the energy is lost. Viscoelastic materials are materials that exhibit both elastic and viscous properties. An underlying assumption in the equations we have developed so far is that the medium in which the waves propagate is purely elastic, and this is also reflected in the conservation of energy.

When deformed by some constant force, an elastic material instantaneously deforms and completely recovers its original shape when the force stops acting on it. Quite opposite, a viscous material would, when being acted on by a constant force, deform until the force stops acting on it, and the deformation does not reverse itself. A viscoelastic material is a material that exhibits a mix of these properties. A rubber band is an example of a very elastic material, a piece of toy clay is an example of a very viscous material, and human tissue is an example of a viscoelastic material. Figure 1 illustrates how the different materials might deform under an impulse force.

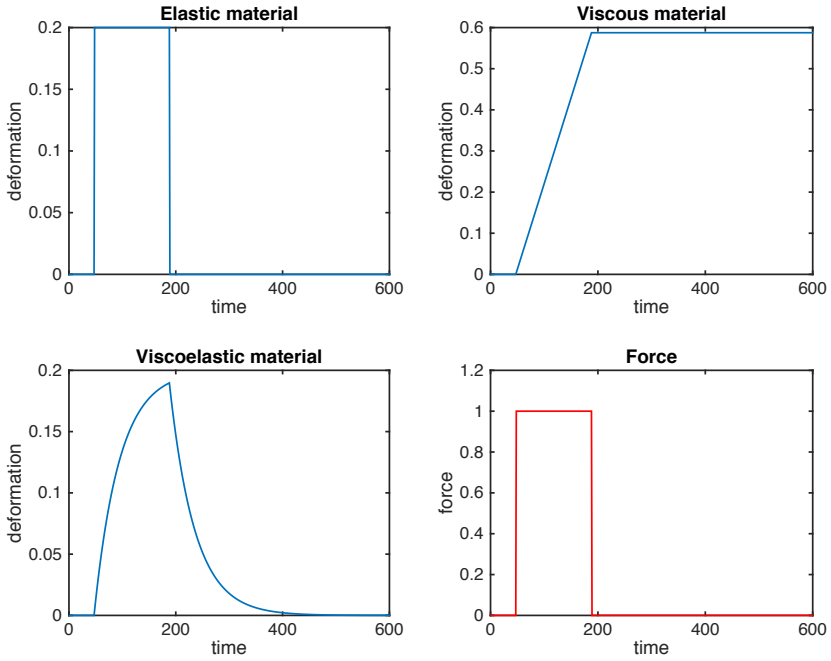

FIGURE 1. On the bottom right, we see the time response of the applied force. The elastic material deforms in agreement with the applied force. The rate of deformation for the viscous material is proportional to the applied force, and hence the material deforms linearly until the force stops acting. The viscoelastic material inherits a combination of these properties, and deforms at at varying rate, before it slowly returns to its initial configuration. Values on axis are arbitrary.

One could attempt to model viscoelastic behavior from the molecular level, but this is a difficult

and intractable problem due to the number of molecules involved. Instead one tries to model the macroscopic behaviour with simpler, heuristic models.

Two important concepts in viscoelastic models are stress and strain. Stress, denoted $\sigma(\mathbf{X},t)$, is a representation of surface forces that particles exert on each other. Strain, denoted $\epsilon(\mathbf{X},t)$, is a measure of the deformation of the material. Both ϵ and σ are represented as tensors. In the case of small deformations and pressure induced forces, they take the form [16]

$$\epsilon(\mathbf{X},t) = \frac{1}{2}(\mathrm{F}^T + \mathrm{F}) - I \qquad \sigma(\mathbf{X},t) = -p\mathrm{I}, \tag{4.22}$$

where $F = \nabla\varphi$ is the deformation gradient. We are mainly interested in the volumetric strain, defined as $\epsilon_v = \mathrm{tr}(\epsilon(\mathbf{X},t)) = \nabla \cdot U$. The viscoelastic equations are given as relations between the components of ϵ and σ, and E and η, the elastic modulus and viscosity parameters, respectively. In the case of pressure induced strain, we have $E = \frac{1}{\kappa_0}$. There exists multiple models to account for viscoelastic effects, but as proposed in [3], the Three-element-model gives an is an adequate model for such effects in soft tissue.

The Three-element-model

In [20] the elastic and viscous pressure-density relations are given in terms of excess density ρ', ambient density ρ_0, compressibility κ_0, the viscosity parameter η and the pressure p. From (3.34) we get the first order approximation $\rho' = -\rho_0 \nabla \cdot U = -\rho_0 \epsilon_v$. The Three-element-model is pictured in Figure 2. The quantities in the model are the nonlinear elastic strain ϵ_1, the linear elastic and viscous strain, ϵ_s and ϵ_d, the sum of these, ϵ_2. From [14] we have that the linear elastic strain-stress relation is

$$\epsilon_s = \frac{1}{E}\sigma_s = -\kappa_0 p, \tag{4.23}$$

the viscous strain stress relation is

$$\frac{\mathrm{d}\epsilon_d}{\mathrm{d}t} = \frac{1}{\eta}\sigma_d = -\frac{1}{\eta}p, \tag{4.24}$$

and the nonlinear elastic relation, which we recognize from (3.41), is

$$\epsilon_1 = -K(p). \tag{4.25}$$

The model is understood by thinking of each infinitesimal volume as a microscopic mechanical system. This system consists of a nonlinear spring connected to a dashpot and a linear spring aligned in a parallel configuration as in Figure 2. A dashpot is also known as a Newtonian damper, and models the viscous part of the system. The spring is the mechanical analogy of Hooke's law, and is the elastic part of the system. The nonlinear spring represents the nonlinear elastic effects of the system, and the dashpot and linear spring the viscoelastic effects.[3] The total volumetric strain for the system is $\epsilon_v = \epsilon_1 + \epsilon_2$. From (4.25) we have that $\epsilon_1 = -K(p)$. For ϵ_2, one assumes that $\epsilon_2 = \epsilon_s = \epsilon_d$. The total strain over the parallel spring and dashpot is the sum of the strain from the spring and the dashpot, as given in equations (4.23) and (4.24) [14]:

$$\sigma = \sigma_s + \sigma_d = \frac{1}{\kappa_0}\epsilon_s + \eta\frac{\mathrm{d}\epsilon_d}{\mathrm{d}t} = \frac{1}{\kappa_0}\epsilon_2 + \eta\frac{\mathrm{d}\epsilon_2}{\mathrm{d}t} \tag{4.26}$$

[3] A dashpot and spring in parallel is known as the Kelvin-Voigt model, and is one of the fundamental models for viscoelastic effects[14].

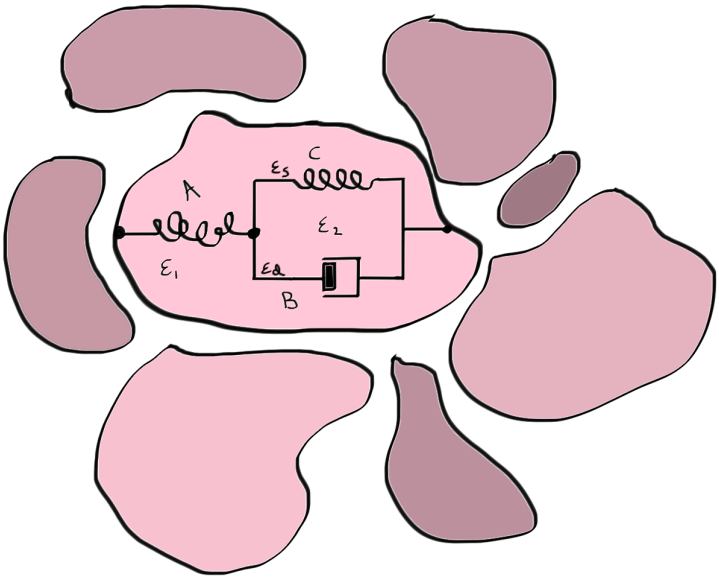

FIGURE 2. Illustration of the Three-element-model. ϵ_1 and ϵ_2 is the volumetric strain in each part of the system, ϵ_s and ϵ_d is the (volumetric) strain in the spring and dashpot part of the parallel part of the system. A is the nonlinear spring, B is the viscous element, the dashpot, and C is the linear spring.

Or, as an ordinary differential equation for ϵ_2, in terms of $\sigma = -p$:

$$\frac{\mathrm{d}\epsilon_2}{\mathrm{d}t} = -\frac{\eta}{\kappa_0}\epsilon_2 - \frac{1}{\eta}p \tag{4.27}$$

Taking the time derivative of ϵ_v, we get

$$\frac{\mathrm{d}\epsilon_v}{\mathrm{d}t} = \frac{\mathrm{d}\epsilon_1}{\mathrm{d}t} + \frac{\mathrm{d}\epsilon_2}{\mathrm{d}t} = -\frac{\mathrm{d}}{\mathrm{d}t}K(p) - \frac{1}{\eta}p - \frac{\eta}{\kappa_0}\epsilon_2. \tag{4.28}$$

Now, since $\frac{\mathrm{d}\epsilon_v}{\mathrm{d}t} = \frac{\partial}{\partial t}\nabla\cdot U = \nabla\cdot V$, and $\frac{\mathrm{d}}{\mathrm{d}t}K(p) = -K'(p)\frac{\partial p}{\partial t}$, we have

$$K'(p)\frac{\partial p}{\partial t} = -\nabla\cdot V - \frac{\eta}{\kappa_0}\epsilon_2 - \frac{1}{\eta}p \tag{4.29}$$

We now have an equation for the acoustic pressure that includes the effect of viscoelastic attenuation. We have added new viscosity term $\epsilon_2 = \varepsilon$, and the ODE (4.27). We continue to look at how attenuation depends on frequency.

Frequency dependent attenuation

The effect of acoustic attenuation is known to be frequency dependent [3, 29], i.e. that the amount of attenuation depends of the vibration frequency of the wave. There are various models to account for this effect in equation (4.29), described in e.g. [14, 4, 8, 31]. We want to adapt the viscoelastic model to include such effects, according to [3]. To explain how this can be done, we do an energy analysis of the viscoelastic system.

When a viscoelastic material is deformed by some periodic function, the stress will generally lag behind the strain. For a sinusoidal volumetric deformation, when the process has reached a steady state, we can assume

$$\epsilon = \epsilon_0 \sin(\omega t) \tag{4.30}$$

where ϵ_0 is an amplitude parameter to be specified. Inserting this expression into the dashpot-spring system in equation (4.27), writing $\sigma = -p$, we get that

$$\sigma = \eta\epsilon_0 \left(\omega \cos(\omega t) + \frac{\eta}{\kappa_0} \sin(\omega t) \right) \tag{4.31}$$

The energy loss during on period of vibration is given as [14]

$$\varepsilon_L = \int_0^{\frac{2\pi}{\omega}} \sigma \mathrm{d}\epsilon. \tag{4.32}$$

Calculation with ϵ and σ as defined above yields

$$\varepsilon_V = \int_0^{\frac{2\pi}{\omega}} \sigma \mathrm{d}\epsilon = \int_0^{\frac{2\pi}{\omega}} \sigma \frac{\mathrm{d}\epsilon}{\mathrm{d}t} \mathrm{d}t = \omega\epsilon_0^2\eta \int_0^{\frac{2\pi}{\omega}} \left(\omega \cos(\omega t) + \frac{\eta}{\kappa_0} \sin(\omega t) \right) \cos(\omega t) \mathrm{d}t = \pi\epsilon_0^2\eta\omega, \tag{4.33}$$

Hence, the attenuation of energy has a linear frequency dependence:

$$\varepsilon_V(\omega) = \pi\eta\omega\epsilon_0^2. \tag{4.34}$$

If one has measurements of the amount of attenuation for specific materials and frequencies, the parameter η could be adjusted to fit the measurements. However, in the continuation of this thesis, we choose to not include this particular loss model. It will be clear that it poses no huge complications or changes in the numerical model to include it, but it is left out since it requires of extra parameters and specific knowledge, in contrast to the rest of the equations, which are more general.

CHAPTER 5

Numerical Method

In this section we propose a numerical method to solve the equations derived in Chapter 3. The method is second order in space and time, and is based of a FDTD[1] method that uses leap frog time integration and staggered grids. The introduction of the Piola-Kirchhoff tensor in (3.29) ads some complexity, but we propose a construction of a staggered grid that handles this without loss of accuracy. The method also uses split-field PML boundary conditions for damping of the waves.

The full system of partial differential equations for the lossless propagation of acoustic waves in two dimensions is

$$\frac{\partial}{\partial t}\begin{bmatrix}U_i\\U_j\end{bmatrix} = \begin{bmatrix}V_i\\V_j\end{bmatrix} \tag{5.1}$$

$$K'(p)\frac{\partial p}{\partial t} = -\frac{\partial V_i}{\partial X} - \frac{\partial V_j}{\partial Y} \tag{5.2}$$

$$\rho_0\frac{\partial}{\partial t}\begin{bmatrix}V_i\\V_j\end{bmatrix} = -\begin{bmatrix}1+\partial_Y U_j & -\partial_Y U_i\\ -\partial_X U_j & 1+\partial_X U_i\end{bmatrix}\begin{bmatrix}\partial_X p\\ \partial_Y p\end{bmatrix}. \tag{5.3}$$

The system (5.1)-(5.3) must be equipped with a suitable set of boundary conditions, initial conditions and as we will see, sources, before we can proceed.

5.1. Sources

An acoustic wave is a propagation of some disturbance from the equilibrium state. This initial disturbance can appear anywhere inside the medium in which the wave propagates, but in the case of a ultrasound wave being exerted into the human body, it would seem natural that the disturbances that cause the incoming wave arises at the boundary of the domain. The disturbance can for example be represented either as a boundary condition on p and V, or as source term in equations (5.2) or (5.3) (or both), included as follows:

$$K'(p)\frac{\partial p}{\partial t} = -\nabla\cdot V + S_m \tag{5.4}$$

$$\rho_0\frac{\partial V}{\partial t} = -\nabla\cdot P + S_F \tag{5.5}$$

We can use the source term S_m to simulate the effect of a vibrating plane. Let a stiff, vibrating plane occupy the region $\Omega_{\mathcal{W}}$, say $\Omega_{\mathcal{W}} = \{(X,Y) : X = a, y_1 \le Y \le y_2\}$, and let $v_p(t)$ be the uniform vibrational speed of the plane, and n its normal vector. We require that $V\cdot n = v_p(t)$, i.e. that the normal velocity is continuous over the plane. Since the vibration causes a local

[1] Finite Difference Time Domain.

change in density, its effect can be modeled as an infinitely thin volume injection source S_m on the form

$$S_m(\mathbf{X},t) = \begin{cases} 2v_p(t)\delta(y-Y) & \text{for } \mathbf{X}, y \in \Omega_{\mathcal{W}} \\ 0 & \text{for } \mathbf{X} \notin \Omega_{\mathcal{W}} \end{cases} \tag{5.6}$$

added to (5.2) [31]. Then S_m produces the same acoustic wave field for $X > a$ as one would get from placing the boundary at $\Omega_{\mathcal{W}}$ enforcing the above mentioned condition on the normal velocity. A source of this type is known as a monopole source. A monopole source source is easiest understood when it acts as a point source. If a infinitesimal spherical volume expands, it displaces its surroundings equally in all directions, and hence initiates a spherical wave.[2] In the case of a monopole plane source, it will radiate two main waves, one in each spatial direction, and also spherical-like waves from the edges of the plane. An example of waves generated by such sources can be seen in Figure 1 and 2. We will later use a source of this type combined with appropriate boundary conditions to generate waves.

FIGURE 1. A 2-D spherical wave from a monopole volume injection point source.

FIGURE 2. A wave from a plane(line) volume injection source.

[2]This is the same kind of wave we looked at in connection with the Lagrangian density.

5.2. Split-field Perfectly Matched Layer

We are interested in the wave-particle interaction, and not reflections or other wave phenomena that occurs at boundaries of our medium. The ideal solution would be to have a infinitely big computational domain, and while we study the region of interest, let the rest of the wave propagate into oblivion. This is of course not computationally feasible, and to remedy this we use a technique called split-field Perfectly Matched Layer. This is not a boundary condition per se, but a modification of the equations to produce a gradual absorption of the wave in certain parts of the computational domain, the Perfectly Matched Layer(PML).

The PML method was initially developed for the equations describing electromagnetic wave propagation [5]. In electrodynamics, both the magnetic and electric fields are vector fields. To use the method in acoustics, one has to split the scalar pressure field into two components, $p = p_i + p_j$, and add them together after computation. Hence the additional "split-field". We will see that the formulation of the equation in terms the components p_i and p_j is natural when we also split $\nabla \cdot V$. The method also has a simpler and more intuitive formulation when used with first order systems like those being treated this thesis, favorable to the more common second order formulations of wave equations like (1.1). In the original paper by *Berenger* [5], the modified equations were introduced, followed by arguments on how and why they worked. Later, others have derived the same equations through rather lengthy arguments on analytical continuation of the wave in to an absorbing infinite space [21]. However, the method appears very intuitive when one sees the modified equations, and we present it as it is given in [23].

We denote our computational domain Ω, and the PML Ω_{pml}, where $\Omega_{pml} \subset \Omega$, and the outer and inner boundaries, Γ_o and Γ_i, are as in Figure 3. We define the absorption coefficients as

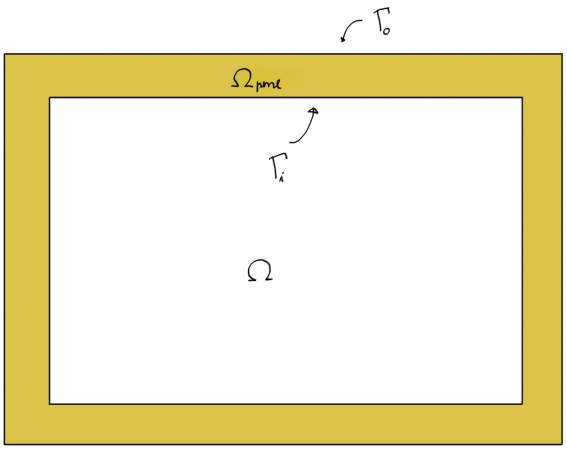

FIGURE 3. A 2-D domain Ω, where the PML-region Ω_{pml} is marked with yellow, and the outer and inner boundaries are Γ_o and Γ_i.

$$\sigma_k(\mathbf{X}) = \begin{cases} \alpha_k(\mathbf{X}) & \text{for } \mathbf{X} \in \Omega_{pml} \\ 0 & \text{for } \mathbf{X} \notin \Omega_{pml} \end{cases} \qquad k = i, j \tag{5.7}$$

where α_k is a positive, real valued function that monotonously increases from 0 to some value α_{max} from Γ_i to Γ_o in Ω_{pml}. The modified equations[3] now become

$$\frac{\partial V_i}{\partial t} = -\frac{1}{\rho_0}\left((1+\partial_Y U_j)\partial_X p - \partial_Y U_i \partial_Y p\right) - \sigma_i V_i \tag{5.8}$$

$$\frac{\partial V_j}{\partial t} = -\frac{1}{\rho_0}\left((1+\partial_X U_i)\partial_Y p - \partial_X U_j \partial_X p\right) - \sigma_j V_j \tag{5.9}$$

$$\frac{\partial p_i}{\partial t} = -\frac{1}{K'(p)}\frac{\partial V_i}{\partial X} - \sigma_i p_i \tag{5.10}$$

$$\frac{\partial p_j}{\partial t} = -\frac{1}{K'(p)}\frac{\partial V_j}{\partial Y} - \sigma_j p_j \tag{5.11}$$

$$p = p_i + p_j \tag{5.12}$$

That the split-field system is equivalent to the original system inside the non-PML region, is easily seen by adding the equations for p_i and p_j. Each of the modified equations roughly resemble equations of the form $g'(\xi) = f(\xi) - \alpha g(\xi)$, where the solution is of the form

$$g(\xi) = c_1 e^{-\alpha\xi} + e^{-\alpha\xi}\int_1^{\xi} f(y)e^{\alpha y}\mathrm{d}y, \tag{5.13}$$

and one sees that the additional term introduces a exponential decay proportional to α. Thus, one obtains a damping of both the velocity and the pressure when inside the PML. This is also intuitively understood since the addition of the PML terms is equivalent to saying that the rate of change of a quantity is equivalent to the negative value of that quantity(plus the contribution from the pressure gradient) when inside the PML. The absorption coefficients have to be specified to yield a gradually increasing damping as the wave propagates through the PML. Sharp changes in absorption can lead to unwanted reflections of the wave, and should be avoided [31]. If we were in 1-D, and the PML was located at $x_1 \leq X \leq x_2$, we could e.g. define

$$\sigma(X) = \begin{cases} \alpha_{max}(x_1 - X)^2 & \text{for } x_1 \leq X \leq x_2 \\ 0 & \text{for } 0 < X < x_1 \end{cases} \tag{5.14}$$

and the parameter α_{max} would need to be set an optimized according to the width of the PML, pressure amplitude, etc. This kind of damping of a sine-wave can be seen in Figure 4.

When the wave enters the PML it becomes increasingly attenuated as it propagates through it, but it does not vanish completely. Hence we need to specify a boundary condition at the outer boundaries of the PML, Γ_o. It is then common to use a Dirichlet boundary condition on the velocity: $V(\mathbf{X}, t) = 0$ on Γ_o, while the pressure at the boundary remains unspecified. Zero vibration velocity means that the boundary is perfectly rigid, and this yields a total reflection of the wave back in to the PML. However, as the reflected wave is also absorbed on its way back from the boundary, it practically becomes negligible.

[3] We don't include the equation for the displacement, as it is unaltered by PML.

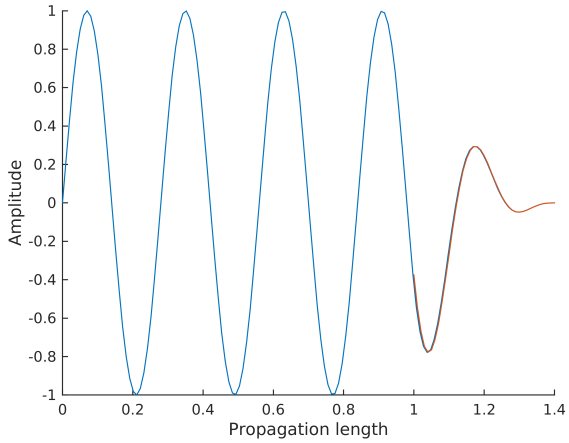

FIGURE 4. A sine wave propagates a unit length before entering the PML. The PML starts where the line color switches from blue to orange, and the amplitude is quickly attenuated.

To initiate waves into Ω, we use a volume injection source as described above in (5.6), placed along a part of the inner boundary Γ_i where we want e.g. a transducer to appear. Hence the part of the wave created by the monopole source S_m not propagating into Ω is immediately absorbed as it propagates into the PML. A graphical explanation of the PML method can been seen in Figure 5, and a simulation of the source/PML combination is seen in Figure 6.

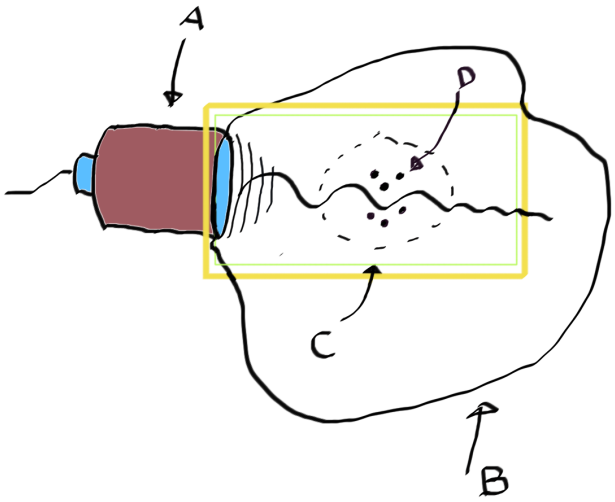

FIGURE 5. A is the ultrasound transducer, the source of the acoustic waves. B can be the entire physical region, while C is our computational domain. The region of interest D is inside the dotted circle. The PML is the area between the thin green rectangle and the broader yellow rectangle, and the source S_m is placed at the inner boundary of the PML, where the blue front end of the transducer is.

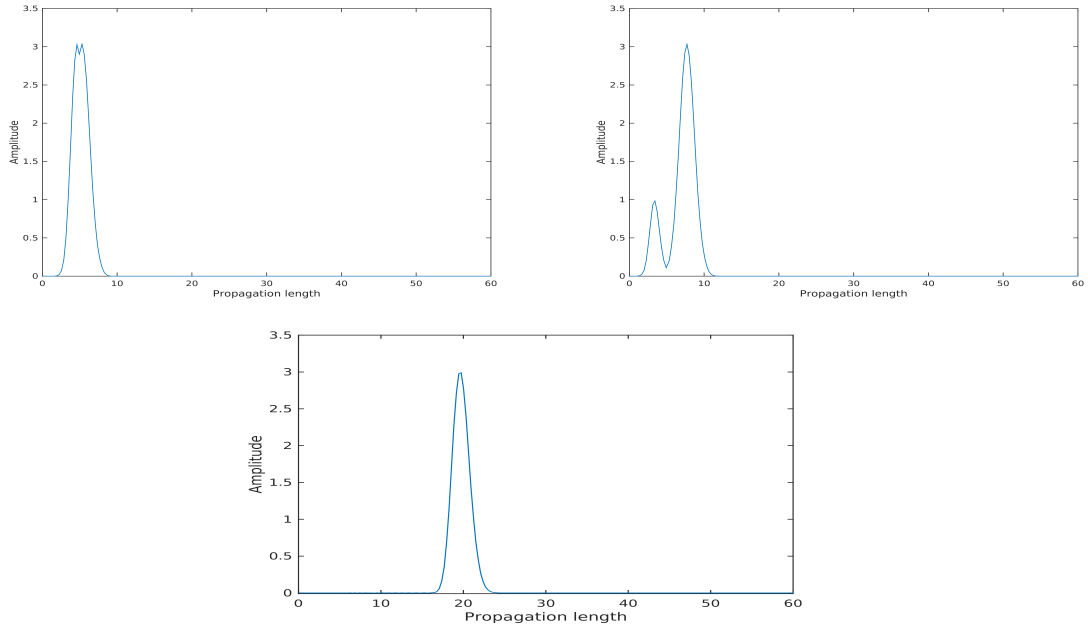

FIGURE 6. A cross section of a Gaussian plane wave radiated by a volume injection source just inside Γ_i. The monopole source radiates two main waves, one traveling in to the domain, and one traveling out of it. The outwards traveling wave quickly absorbs in the PML, while the inwards traveling wave is free to propagate undisturbed. Values on axes are arbitrary.

We assume the medium initially is at equilibrium, i.e. all acoustic quantities are zero. With initial and boundary conditions, PML-modification and addition of sources, the full 2-D system of equations to be solved numerically is

$$\frac{\partial U_i}{\partial t} = V_i \tag{5.15a}$$

$$\frac{\partial U_j}{\partial t} = V_j \tag{5.15b}$$

$$\frac{\partial V_i}{\partial t} = -\frac{1}{\rho_0}\left((1+\partial_Y U_j)\partial_X p - \partial_Y U_i \partial_Y p\right) - \sigma_i V_i \tag{5.15c}$$

$$\frac{\partial V_j}{\partial t} = -\frac{1}{\rho_0}\left((1+\partial_X U_i)\partial_Y p - \partial_X U_j \partial_X p\right) - \sigma_j V_j \tag{5.15d}$$

$$\frac{\partial p_i}{\partial t} = -\frac{1}{K'(p)}\left(\frac{\partial V_i}{\partial X} - \frac{1}{2}S_m\right) - \sigma_i p_i \tag{5.15e}$$

$$\frac{\partial p_j}{\partial t} = -\frac{1}{K'(p)}\left(\frac{\partial V_j}{\partial Y} - \frac{1}{2}S_m\right) - \sigma_j p_j \tag{5.15f}$$

$$p = p_i + p_j \tag{5.15g}$$

$$U, V, p \in \Omega \quad \text{and} \quad U = V = p = 0 \quad \text{at} \quad t = 0$$

$$V_i = V_j = 0 \quad \text{on} \quad \partial\Gamma_o$$

5.3. Discretization

We want to solve the equations (5.15) using a finite difference method in both the spatial and temporal domain. A well known and elegant numerical method used on equations originating from conservation laws involves writing the system in a matrix form and diagonalizing it before solving it, as described in [24, 27]. One problem with this approach is that it gets increasingly complex as the number of dimensions increase and nonlinear terms are added. In [31], a number of numerical methods for solving the linear equations (2.4) and (2.6) are proposed, e.g. finite element methods, pseudospectral methods and finite difference methods. One of the finite difference methods, a method also originating from the field of electrodynamics,[4] combines a grid construction technique called staggered grid, and a time integration method known as leapfrog time integration, where different quantities are computed at alternating time steps. We propose a finite difference scheme based on the same idea, but first we examine the method in its original form to see how it works on the linear and nonlinear Eulerian equations, (2.4), (2.6),(2.15) and (2.15), and why it fails on (5.15).

Leapfrog on Staggered Grid for the Eulerian equations

We start by defining discrete variables. Let $\Omega_{I,J} = \{(x_i, y_i) = (i\Delta x, j\Delta y), i, j \in \mathbb{N}, 0 \leq i \leq I, 0 \leq j \leq J\}$ be the discrete domain, where I and J are the number of nodes in the x and y-direction, respectively. We let $\Delta x = \frac{L_x}{I}$ and $\Delta y = \frac{L_y}{J}$, where L_x and L_y are the domain lengths in the x and y-direction. The discrete time is denoted t_n, where $t_n = n\Delta t$ and $n \in \mathbb{N}$, and Δt is some chosen temporal step length. We denote discrete function values as

$$
\begin{aligned}
f(x_i, y_j, t_n) &= f(i\Delta x, j\Delta y, n\Delta t) = f^n_{i,j} \\
f(x_i, y_j, t_{n+\frac{1}{2}}) &= f(i\Delta x, j\Delta y, n\Delta t + \frac{1}{2}\Delta t) = f^{n+\frac{1}{2}}_{i,j} \\
f(x_{i+\frac{1}{2}}, y_j, t_n) &= f(i\Delta x + \frac{1}{2}\Delta x, j\Delta y, n\Delta t) = f^n_{i+\frac{1}{2},j} \qquad \text{etc.}
\end{aligned}
$$

The idea behind the leapfrog time integration is to solve the equations for p and v at different timesteps. One uses p^n to compute $v^{n+\frac{1}{2}}$, and $v^{n+\frac{1}{2}}$ to compute p^{n+1} and so forth. The staggered grid in the spatial domain places the nodes such that spatial derivatives at $f^n_{i,j}$ are computed from neighboring points, a half step away in the x and y-directions, by a second order central difference operator. More specifically, we approximate the temporal and spatial derivatives as

$$
\begin{aligned}
\left.\frac{\partial f}{\partial x}\right|^n_{(i,j)} &= \frac{f^n_{i+\frac{1}{2},j} - f^n_{i-\frac{1}{2},j}}{\Delta x} + \mathcal{O}(\Delta x^2) \\
\left.\frac{\partial f}{\partial y}\right|^n_{(i,j)} &= \frac{f^n_{i,j+\frac{1}{2}} - f^n_{i,j-\frac{1}{2}}}{\Delta y} + \mathcal{O}(\Delta y^2) \\
\left.\frac{\partial f}{\partial t}\right|^n_{(i,j)} &= \frac{f^{n+\frac{1}{2}}_{i,j} - f^{n-\frac{1}{2}}_{i,j}}{\Delta x} + \mathcal{O}(\Delta t^2)
\end{aligned}
$$

[4] The first paper on the method seems to be "Numerical solution of initial boundary value problems involving Maxwell's equations in isotropic media" [32], written by *Kane Yee*.

The computational molecules in Figure 7 shows how the nodes are aligned and used in the computation, and Figure 8 shows a section of the staggered grid. It works very elegantly due to the structure of the system: (2.4) and (2.6) constitutes a mixed system, where the temporal derivative of p depends on the divergence of v and vice versa, and the staggered grid lets us compute $p_{i,j}^{n+1}$ from the divergence of $v_{i,j}^{n+\frac{1}{2}}$, which is computed from the nodes surrounding (x_i, y_j). The same technique applies to computation of the velocity components from the pressure gradient. The discretization of (2.4) and (2.6), with $v = [u, v]^T$ becomes

$$\frac{p_{i,j}^{n+1} - p_{i,j}^{n}}{\Delta t} = -\frac{1}{\kappa_0} \frac{u_{i+\frac{1}{2},j}^{n+\frac{1}{2}} - u_{i-\frac{1}{2},j}^{n+\frac{1}{2}}}{\Delta x} - \frac{1}{\kappa_0} \frac{v_{i,j+\frac{1}{2}}^{n+\frac{1}{2}} - v_{i,j-\frac{1}{2}}^{n+\frac{1}{2}}}{\Delta y} \tag{5.16}$$

$$\frac{u_{i+\frac{1}{2},j}^{n+\frac{1}{2}} - u_{i+\frac{1}{2},j}^{n-\frac{1}{2}}}{\Delta t} = -\frac{1}{\rho_0} \frac{p_{i+1,j}^{n} - p_{i,j}^{n}}{\Delta x} \tag{5.17}$$

$$\frac{v_{i,j+\frac{1}{2}}^{n+\frac{1}{2}} - v_{i,j+\frac{1}{2}}^{n-\frac{1}{2}}}{\Delta t} = -\frac{1}{\rho_0} \frac{p_{i,j+1}^{n} - p_{i,j}^{n}}{\Delta y} \tag{5.18}$$

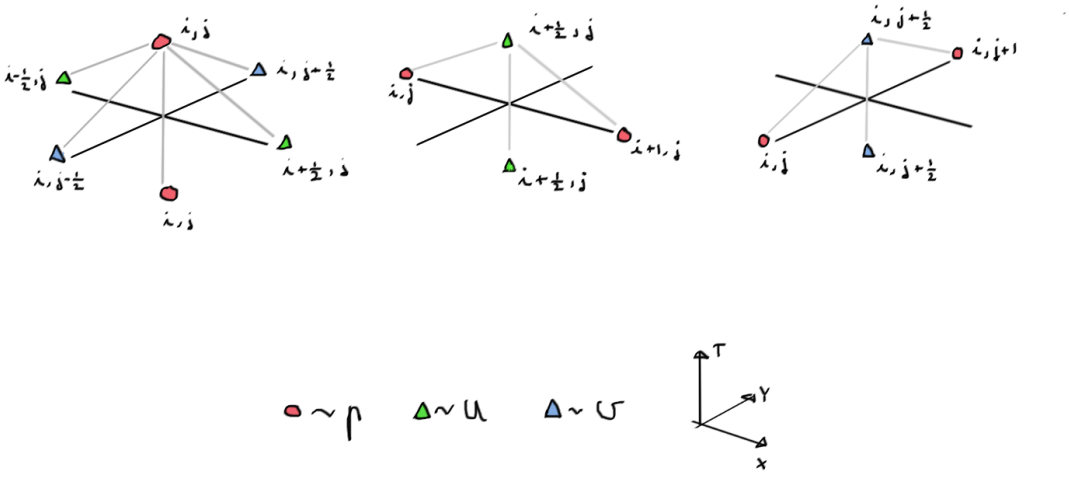

FIGURE 7. Computational molecules for p, u and v according to the discretization in equations (5.16)-(5.18).

As we mentioned, the central difference operators used in this discretization are second order approximations to the analytic derivatives, meaning that truncated terms in the approximation occur with a factor $\Delta x^m = (\Delta x)^m$, where $m \geq 2$. In numerical methods solving wave equations,

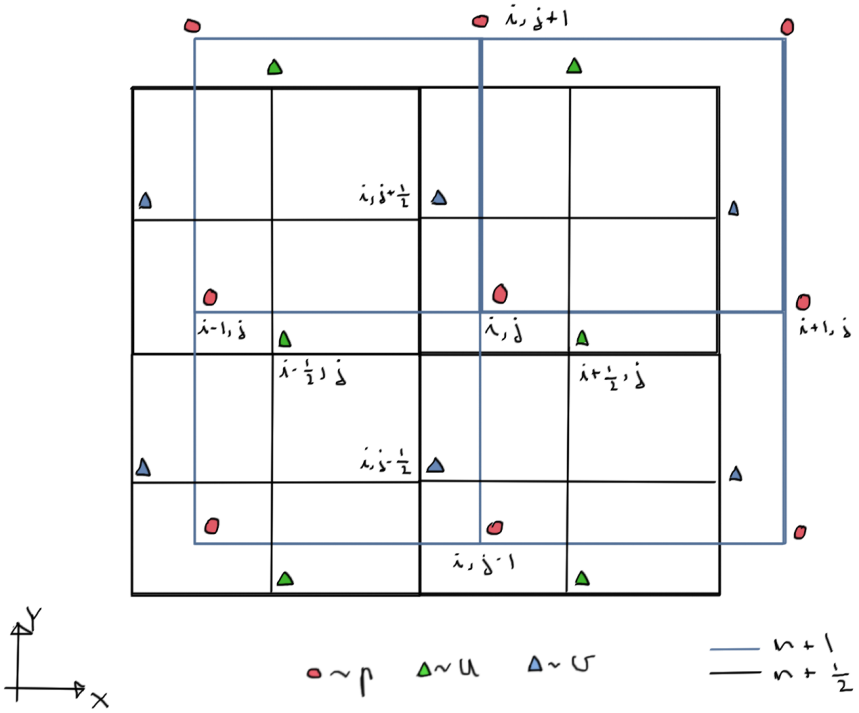

FIGURE 8. Section of the staggered grid.

this feature is important, as first order approximations of spatial derivatives adds unwanted numerical diffusion to the the solution. Expanding a forward difference operator of a spatial derivative in a Taylor series shows why:

$$\frac{1}{\Delta x}\left(f^n_{i+1,j} - f^n_{i,j}\right) = \left.\frac{\partial f}{\partial x}\right|^n_{(i,j)} + \frac{1}{2}\Delta x \left.\frac{\partial^2 f}{\partial x^2}\right|^n_{(i,j)} + \mathcal{O}(\Delta x^2) \tag{5.19}$$

Hidden in the first order approximation is the second spatial derivative. Hence, using a first order forward difference operator in a equation like (2.4) would compare to solving the equation

$$\frac{\partial p}{\partial t} \approx -\frac{1}{\kappa_0}\left(\nabla \cdot v + \frac{1}{2}\Delta x \nabla^2 v\right) + \mathcal{O}(\Delta x^2), \tag{5.20}$$

where the term $\frac{1}{2}\Delta x \nabla^2 v$ is recognized as a diffusion term appearing in the heat equation or in transport equations [26]. Diffusion, manifested as a smoothing and "spreading out" of the solution as seen in Figure 9, is avoided by using the central difference operator. By a Taylor expansion we get

$$\frac{f^n_{i+\frac{1}{2},j} - f^n_{i-\frac{1}{2},j}}{\Delta x} = \left.\frac{\partial f}{\partial x}\right|^n_{(i,j)} + \frac{1}{24}\Delta x^2 \left.\frac{\partial^3 f}{\partial x^3}\right|^n_{(i,j)} + \mathcal{O}(\Delta x^3). \tag{5.21}$$

There is no diffusive term hidden this approximation. Hence, we want to use second order operators in our method.

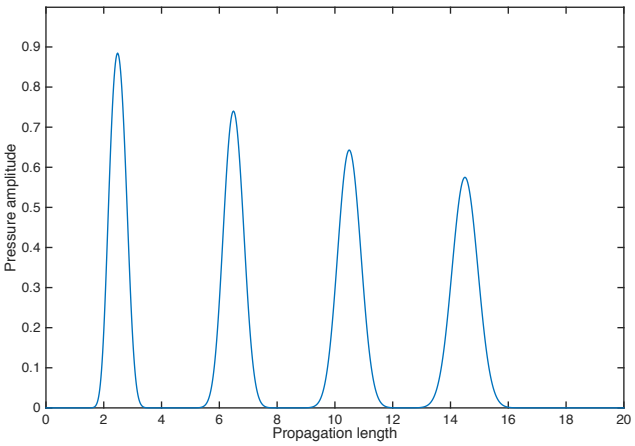

FIGURE 9. Plot of from a 1-D implementation of a first order upwinding scheme. One sees how the numerical diffusion attenuates and spreads out a pressure wave.

The scheme presented above can easily be used for the nonlinear equations (2.15) and (2.17), when neglecting the Lagrangian density. We only have to change the scheme for the pressure equation, using a explicit variation of the central difference operator, to get

$$\frac{p_i^{n+1}-p_i^n}{\Delta t} = -\frac{1}{K'(p_{i,j}^n)}\left(\frac{u_{i+\frac{1}{2},j}^{n+\frac{1}{2}}-u_{i-\frac{1}{2},j}^{n+\frac{1}{2}}}{\Delta x}+\frac{v_{i,j+\frac{1}{2}}^{n+\frac{1}{2}}-v_{i,j-\frac{1}{2}}^{n+\frac{1}{2}}}{\Delta y}\right), \tag{5.22}$$

where $K'(p_{i,j}^n) = \kappa_0 - \beta\kappa_0^2 p_{i,j}^n$.

Leapfrog on Staggerd Grid for the Lagrangian equations

We now want to apply a similar method to the Lagrangian equations. A closer look at e.g. the momentum equation (5.15)c-d reveals that the grid structure used for the Eulerian equations is not well suited: if we consider the component V_i, we have that

$$\rho_0\frac{\partial V_i}{\partial t} = -\left((1+\partial_Y U_j)\partial_X p - \partial_Y U_i \partial_Y p\right). \tag{5.23}$$

First, we see that the equation includes the displacement U, and hence this quantity also has to live at some suitable set of nodes. Second, it depends on the pressure gradient in both the x and y-direction, but as we see from Figure 8, a velocity component $(V_i)_{i,j}$ is not placed in a way that lets us apply the central difference in a natural way to obtain this. To fix this, and allow the leapfrog time integration, we need a grid that satisfies the following requirements:

- The pressure and displacement nodes are placed such that we can compute spatial gradients with central differences in a natural way when computing velocity components.

- The pressure and displacement nodes should be computed at the same timestep.
- The the velocity nodes should be placed such that when we compute velocity gradients at pressure nodes, it can be done using the central difference operator.

To meet these requirements, we propose the grid shown in Figure 10.

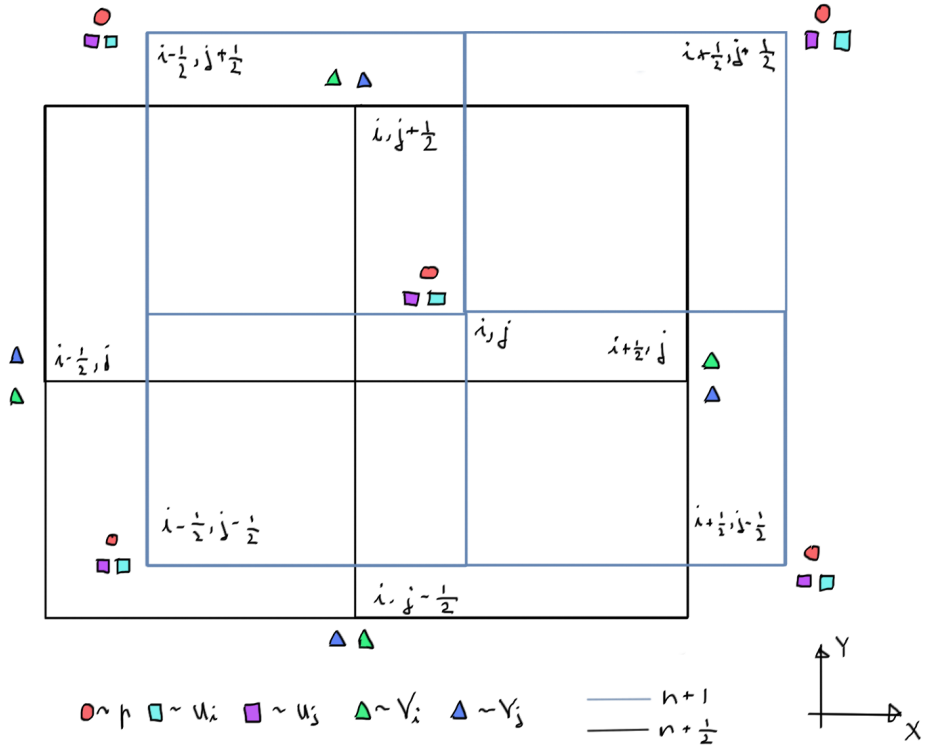

FIGURE 10. A staggered grid structure for the Lagrangian equations. It differs from the grid in Figure 8, both in that it contains displacement values U_i,U_j and in the relative positioning of the nodes.

As we will see, with this grid construction, central difference operators can be used in a natural way in both space and time, and by computing p and U in the same time step, and V at the next, the leapfrog time integration can be used similarly as with the Eulerian equations. It might seem strange that the velocity and displacement does not reside at the same nodes, but there is really no need for this, as in the limit when increments go to zero, all approximations will remain consistent with the original equations. The computational molecules for U_i, V_i and p are shown in Figure 11. We now give a detailed exposition of the discretization used in solving each of the equations in (5.15), starting with the displacement:

$$\frac{\partial U_i}{\partial t} = V_i \qquad \frac{\partial U_j}{\partial t} = V_j \tag{5.24}$$

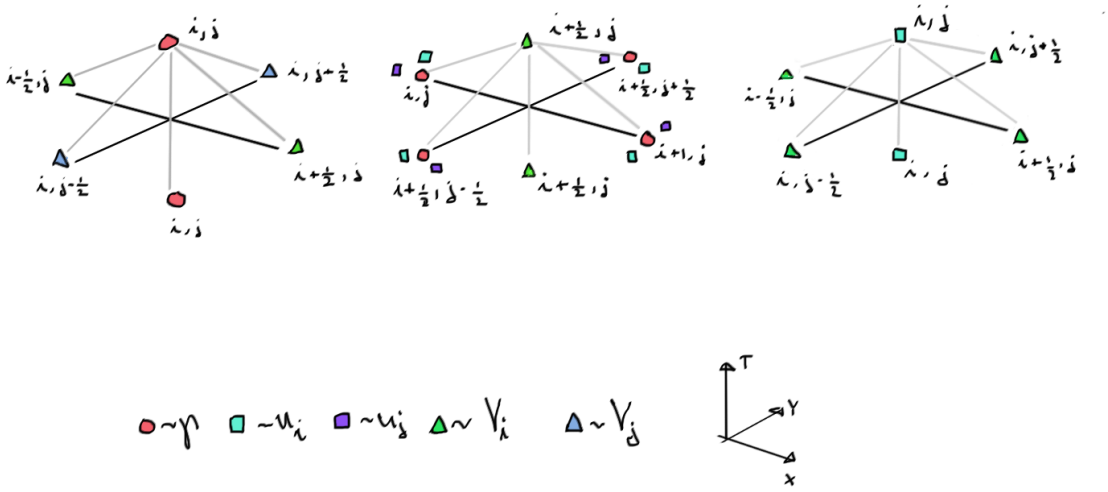

FIGURE 11. Computational molecules for central difference operators on the grid in Figure 10.

$$\left.\frac{\partial U_i}{\partial t}\right|_{(i,j)}^{n+\frac{1}{2}} \approx \frac{(U_i)_{i,j}^{n+1} - (U_i)_{i,j}^{n}}{\Delta t} \qquad \left.\frac{\partial U_j}{\partial t}\right|_{(i,j)}^{n+\frac{1}{2}} \approx \frac{(U_j)_{i,j}^{n+1} - (U_j)_{i,j}^{n}}{\Delta t}$$

$$V_i\Big|_{(i,j)}^{n+\frac{1}{2}} \approx \frac{1}{4}\left((V_i)_{i+\frac{1}{2},j}^{n+\frac{1}{2}} + (V_i)_{i-\frac{1}{2},j}^{n+\frac{1}{2}} + (V_i)_{i,j+\frac{1}{2}}^{n+\frac{1}{2}} + (V_i)_{i,j-\frac{1}{2}}^{n+\frac{1}{2}}\right)$$

$$V_j\Big|_{(i,j)}^{n+\frac{1}{2}} \approx \frac{1}{4}\left((V_j)_{i+\frac{1}{2},j}^{n+\frac{1}{2}} + (V_j)_{i-\frac{1}{2},j}^{n+\frac{1}{2}} + (V_j)_{i,j+\frac{1}{2}}^{n+\frac{1}{2}} + (V_j)_{i,j-\frac{1}{2}}^{n+\frac{1}{2}}\right)$$

For the split-field pressure components we have

$$K'(p)\frac{\partial p_i}{\partial t} = -\frac{\partial V_i}{\partial X} \qquad K'(p)\frac{\partial p_j}{\partial t} = -\frac{\partial V_j}{\partial Y} \qquad p = p_i + p_j \tag{5.25}$$

$$K'(p)\left.\frac{\partial p_i}{\partial t}\right|_{(i,j)}^{n+\frac{1}{2}} \approx K'(p_{i,j}^n)\frac{(p_i)_{i,j}^{n+1} - (p_i)_{i,j}^{n}}{\Delta t} \qquad \left.\frac{\partial V_i}{\partial X}\right|_{(i,j)}^{n+\frac{1}{2}} = \frac{(V_i)_{i+\frac{1}{2},j}^{n+\frac{1}{2}} - (V_i)_{i-\frac{1}{2},j}^{n+\frac{1}{2}}}{\Delta X}$$

$$K'(p)\left.\frac{\partial p_j}{\partial t}\right|_{(i,j)}^{n+\frac{1}{2}} \approx K'(p_{i,j}^n)\frac{(p_j)_{i,j}^{n+1} - (p_j)_{i,j}^{n}}{\Delta t} \qquad \left.\frac{\partial V_j}{\partial Y}\right|_{(i,j)}^{n+\frac{1}{2}} = \frac{(V_j)_{i,j+\frac{1}{2}}^{n+\frac{1}{2}} - (V_j)_{i,j-\frac{1}{2}}^{n+\frac{1}{2}}}{\Delta Y}$$

And for the momentum equation we have

$$\rho_0 \frac{\partial V_i}{\partial t} = -\left((1+\partial_Y U_j)\partial_X p - \partial_Y U_i \partial_Y p\right) \tag{5.26}$$

$$\rho_0 \frac{\partial V_j}{\partial t} = -\left((1+\partial_X U_i)\partial_Y p - \partial_X U_j \partial_X p\right) \tag{5.27}$$

$$\left.\frac{\partial V_i}{\partial t}\right|^n_{(i+\frac{1}{2},j)} \approx \frac{(V_i)^{n+\frac{1}{2}}_{i+\frac{1}{2},j} - (V_i)^{n-\frac{1}{2}}_{i+\frac{1}{2},j}}{\Delta t} \qquad \left.\frac{\partial V_j}{\partial t}\right|^n_{(i+\frac{1}{2},j)} \approx \frac{(V_j)^{n+\frac{1}{2}}_{i+\frac{1}{2},j} - (V_j)^{n-\frac{1}{2}}_{i+\frac{1}{2},j}}{\Delta t}$$

$$\left.\frac{\partial U_i}{\partial X}\right|^n_{(i+\frac{1}{2},j)} \approx \frac{(U_i)^n_{i+1,j} - (U_i)^n_{i,j}}{\Delta X} \qquad \left.\frac{\partial U_j}{\partial X}\right|^n_{(i+\frac{1}{2},j)} \approx \frac{(U_j)^n_{i+1,j} - (U_j)^n_{i,j}}{\Delta X}$$

$$\left.\frac{\partial U_i}{\partial Y}\right|^n_{(i+\frac{1}{2},j)} \approx \frac{(U_i)^n_{i+\frac{1}{2},j+\frac{1}{2}} - (U_i)^n_{i+\frac{1}{2},j-\frac{1}{2}}}{\Delta Y} \qquad \left.\frac{\partial U_j}{\partial Y}\right|^n_{(i+\frac{1}{2},j)} \approx \frac{(U_j)^n_{i+\frac{1}{2},j+\frac{1}{2}} - (U_j)^n_{i+\frac{1}{2},j-\frac{1}{2}}}{\Delta Y}$$

$$\left.\frac{\partial p}{\partial X}\right|^n_{(i+\frac{1}{2},j)} \approx \frac{p^n_{i,j} - p^n_{i+1,j}}{\Delta X} \qquad \left.\frac{\partial p}{\partial Y}\right|^n_{(i+\frac{1}{2},j)} \approx \frac{p^n_{i+\frac{1}{2},j+\frac{1}{2}} - p^n_{i+\frac{1}{2},j-\frac{1}{2}}}{\Delta Y}$$

By the same method as in (5.21) one can easily verify that all the approximations above are second order.
Combining the above discretizations and adding sources and the PML-modification, we get a numerical scheme that is second order both in space and time:

$$(V_i)^{n+\frac{1}{2}}_{i+\frac{1}{2},j} = (V_i)^{n-\frac{1}{2}}_{i+\frac{1}{2},j} - \frac{\Delta t}{(\rho_0)_{i+\frac{1}{2},j}}\left(1 + \frac{(U_j)^n_{i+\frac{1}{2},j+\frac{1}{2}} - (U_j)^n_{i+\frac{1}{2},j-\frac{1}{2}}}{\Delta Y}\right)\frac{p^n_{i,j} - p^n_{i+1,j}}{\Delta X}$$
$$+\frac{\Delta t}{(\rho_0)_{i+\frac{1}{2},j}}\left(\frac{(U_i)^n_{i+\frac{1}{2},j+\frac{1}{2}} - (U_i)^n_{i+\frac{1}{2},j-\frac{1}{2}}}{\Delta Y}\right)\frac{p^n_{i+\frac{1}{2},j+\frac{1}{2}} - p^n_{i+\frac{1}{2},j-\frac{1}{2}}}{\Delta Y} - \Delta t(\sigma_i)_{i,j}(V_i)^{n-\frac{1}{2}}_{i+\frac{1}{2},j}$$

$$(V_j)^{n+\frac{1}{2}}_{i+\frac{1}{2},j} = (V_j)^{n-\frac{1}{2}}_{i+\frac{1}{2},j} - \frac{\Delta t}{(\rho_0)_{i+\frac{1}{2},j}}\left(1 + \frac{(U_i)^n_{i+1,j} - (U_i)^n_{i,j}}{\Delta X}\right)\frac{p^n_{i+\frac{1}{2},j+\frac{1}{2}} - p^n_{i+\frac{1}{2},j-\frac{1}{2}}}{\Delta Y}$$
$$+\frac{\Delta t}{(\rho_0)_{i+\frac{1}{2},j}}\left(\frac{(U_j)^n_{i+1,j} - (U_j)^n_{i,j}}{\Delta X}\right)\frac{p^n_{i,j} - p^n_{i+1,j}}{\Delta X} - \Delta t(\sigma_j)_{i,j}(V_j)^{n-\frac{1}{2}}_{i+\frac{1}{2},j}$$

$$(p_i)_{i,j}^{n+1} = (p_i)_{i,j}^n - \frac{\Delta t}{K'(p_{i,j}^n)} \left(\frac{(V_i)_{i+\frac{1}{2},j}^{n+\frac{1}{2}} - (V_i)_{i-\frac{1}{2},j}^{n+\frac{1}{2}}}{\Delta X} - \frac{1}{2}(S_m)_{i,j}^n \right) - \Delta t(\sigma_i)_{i,j}(p_i)_{i,j}^n$$

$$(p_j)_{i,j}^{n+1} = (p_j)_{i,j}^n - \frac{\Delta t}{K'(p_{i,j}^n)} \left(\frac{(V_j)_{i,j+\frac{1}{2}}^{n+\frac{1}{2}} - (V_j)_{i,j-\frac{1}{2}}^{n+\frac{1}{2}}}{\Delta Y} - \frac{1}{2}(S_m)_{i,j}^n \right) - \Delta t(\sigma_i)_{i,j}(p_j)_{i,j}^n$$

$$p_{i,j}^{n+1} = (p_i)_{i,j}^{n+1} + (p_j)_{i,j}^{n+1}$$

$$(U_i)_{i,j}^{n+1} = (U_i)_{i,j}^n + \frac{\Delta t}{4} \left((V_i)_{i+\frac{1}{2},j}^{n+\frac{1}{2}} + (V_i)_{i-\frac{1}{2},j}^{n+\frac{1}{2}} + (V_i)_{i,j+\frac{1}{2}}^{n+\frac{1}{2}} + (V_i)_{i,j-\frac{1}{2}}^{n+\frac{1}{2}} \right)$$

$$(U_j)_{i,j}^{n+1} = (U_j)_{i,j}^n + \frac{\Delta t}{4} \left((V_j)_{i+\frac{1}{2},j}^{n+\frac{1}{2}} + (V_j)_{i-\frac{1}{2},j}^{n+\frac{1}{2}} + (V_j)_{i,j+\frac{1}{2}}^{n+\frac{1}{2}} + (V_j)_{i,j-\frac{1}{2}}^{n+\frac{1}{2}} \right)$$

A MATLAB implementation of this scheme, written to preform the numerical experiment i Chapter 6, can be found in the appendix. The code also contains a modification of the scheme that allows for comparison with the Eulerian equations.

Properties of the scheme

To say something about the properties of the numerical scheme proposed above is difficult. The very essential property that the discrete equations are consistent with the continuous equations can easily be established. But one also wants to know if the scheme is stable, and if it converges. The scheme should be stable in the sense that numerical errors do not increase with time. That the scheme is convergent means that the numerical solutions tends to the actual solution as discrete increments tend to zero. Also, if conservation laws hold for the system, one should investigate if the numerical scheme satisfies these.
In the paper describing the original method [32], a stability criterion that resembles a CFL-condition is given, without any rigorous analysis, and this should hold for the linear Eulerian method too. The criterion says that the method is stable if

$$\sqrt{\Delta x^2 + \Delta y^2} > C\Delta t,$$

where Δx,Δy and Δt are discrete increments as defined above, and $C = C_1 \max_{x \in \Omega}(c_0(x))$ with $0 \leq C_1 \leq 1$, i.e. C is the maximum wave propagation velocity inside the domain. This similar to the CFL-condition for hyperbolic PDEs, and has the natural interpretation that information should not travel more than one discrete length, or cell length, per time step [27]. Experimentation with the scheme shows that $C_1 \leq \frac{1}{3}$ hinders unwanted numerical oscillations.
It is not whitin the scope of this thesis investigate these properties further, but we can say that from numerical experiments, the numerical scheme seems stable and produces solutions that behaves as one would expect.

Implementation

With the discrete scheme described above, it is convenient to represent the field quantities $U_i, U_j, V_i, V_j, p_i, p_j$ and p as matrices. If a grid size (I, J) is chosen, each of the fields is represented discretely as a matrix $M \in \mathbb{R}^{2I \times 2J}$. The reason for the unfortunate doubling of nodes in each dimension of the discrete field is is due to the structure of the grid; due to the staggered grid and the halfstep difference operators, there is no simple data structure to represent the "square with center" node distribution of p and U, and the interleaved "diamond" node distribution of V. However, the matrix representation of the acoustic fields makes the implementation flexible and lucid. The scheme is also suitable for parallelisation, e.g. to be ran on GPU's (Graphics Processing Unit), as the computational operations are "local", in the sense that computation of values only rely on a small amount of the information. Hence the computation can be split into many local, smaller computations, each preformed separately, and put back together when finished. Due to lack of computer facilities we were not able to implement a parallel version of the scheme.

CHAPTER 6

Numerical experiment

The are a number of scenarios where the Lagrangian equations could give interesting results. We choose to focus on one particular situation, pointed[1] out by *B. A. Angelsen* and *O. F. Myhre* at ISB, NTNU: Scattering of ultrasound from a particle from intersecting waves with different frequencies. When sending waves of different frequencies from orthogonal angles at a small particle, the waves scattered from the particle are easier to observe. The experiment was done in connection with a project by SURF Technology, mentioned in the introduction, where one wants to use a combination of high and low frequency ultrasound waves to detect micro calcium particles in breast tissue. If this is achieved, it is a step towards better methods for detecting breast cancer.

We do simulations of this scenario with both the Lagrangian and Eulerian equations, and point to how this particular example illustrate some of the differences between the Lagrangian and Eulerian equations, and how the Lagrangian equations might be better suited to model it.

6.1. The experiment

A sketch of the experimental setup is given in Figure 1, and the data (frequencies, pressure etc.) is provided by *O. F. Myhre*. We simulate the behavior of the waves in the focus area of the intersecting ultrasound beams, where the waves roughly appear as plane waves. The particle is placed at the center of the domain, and the waves are produced by sources as described in Chapter 5. We continuously excite a sine wave at T_1 with frequency of $f_{LF} = 1$ MHz, and at time t_m we excite a $f_{HF} = 10$ MHz sine wave in a Gaussian envelope from T_2, in the direction orthogonal to the low frequency sine wave. We record the pressure signal at T_2, and denote the recorded signal as P.

The particle is a calcium particle, and the surrounding medium is human fat. Material parameters, found in [3, 31], are given in Table 1.

Material	ρ_0 (kg m^{-3})	κ_0 (m s^2 kg^{-1})	c_0 (m s^{-1})	β (1)
Fat	928	5.3×10^{-10}	1430	6.14
Calcium	1550	4.5×10^{-11}	3810	≈ 0

TABLE 1. Material parameters for fat and calcium.

We let the wavelength of the high frequency wave determine the size of the computational

[1]Explained in conversation. This means we do not have a report with data from the experiment, and to our knowledge no such report exists.

domain Ω.

$$\lambda = \frac{c_0}{f_{HF}} = \frac{1430}{10 \cdot 10^6} \text{ m} = 1.43 \cdot 10^{-4} \text{ m} = 143 \ \mu\text{m} \tag{6.1}$$

We choose Ω to be $3000 \ \mu\text{m} \times 3000 \ \mu\text{m}$. This allows the high frequency wave to propagate for some time, about 10 wavelengths, before it hits the particle. The particle diameter varies from $20 - 300 \ \mu$m, and in the MATLAB script we allow for square, triangular and circular particle geometry. The vibration speed for the sources are

$$v_{LF}(t) = \frac{p_0}{z_0} \sin(2\pi f_{LF} t) \quad \text{and} \quad v_{HF}(t) = \frac{p_0}{z_0} \sin(2\pi f_{HF} t) \exp\left(-\frac{(t - t_m)^2}{2\sigma^2} \right), \tag{6.2}$$

where $z_0 = \rho_0 c_0$ is the plane wave impedance, and $\sigma = \frac{3}{4.3 f_{HF}}$ determines the width of the Gaussian envelope on the high frequency wave, and is set to approximately three wavelengths. p_0 is in the pressure of the incoming wave, and we use $p_0 = 2$MPa.

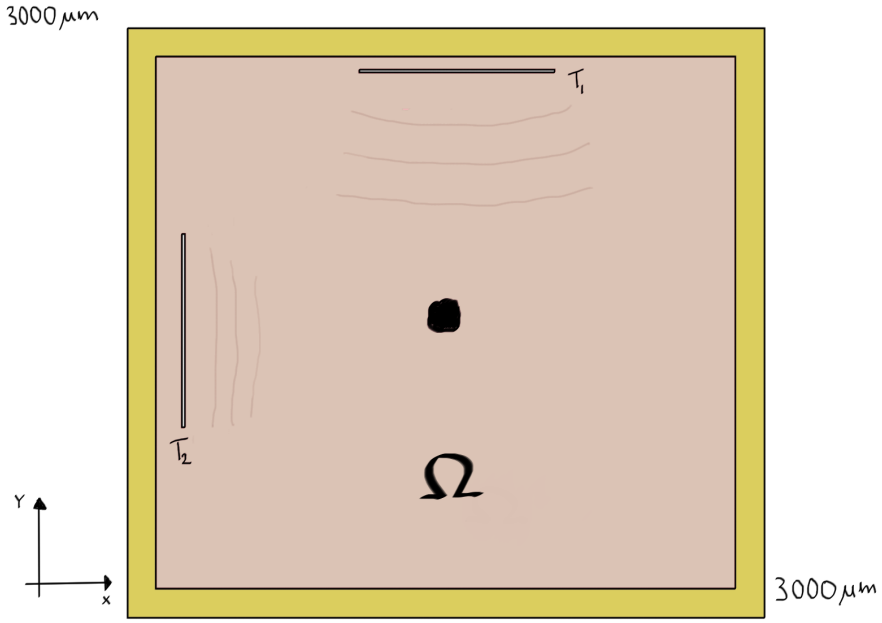

FIGURE 1. Sketch of the experimental setup. Ω is the computational domain, with the particle at the center. The low frequency wave propagates from T_1, while the high frequency wave propagates from T_2. We continuously record the signal at T_2, so both the outgoing and incoming signal from the high frequency wave is recorded.

What can we expect to see from this experiment? Since the particle is stiffer and heavier than its surroundings, and the low frequency wave exert a periodic radiation force on it, it might start to vibrate out of phase with its surroundings, causing a rapid variation in displacement

and density [3]. When we compare the Eulerian[2] and Lagrangian momentum equations,

$$\rho_0 \frac{\partial}{\partial t} \begin{bmatrix} v_i \\ v_j \end{bmatrix} = - \begin{bmatrix} \partial_x p \\ \partial_y p \end{bmatrix} \tag{6.3}$$

$$\rho_0 \frac{\partial}{\partial t} \begin{bmatrix} V_i \\ V_j \end{bmatrix} = - \begin{bmatrix} 1+\partial_Y U_j & -\partial_Y U_i \\ -\partial_X U_j & 1+\partial_X U_i \end{bmatrix} \begin{bmatrix} \partial_X p \\ \partial_Y p \end{bmatrix}, \tag{6.4}$$

we see that such variation in displacement enters in the Lagrangian equation, through components of the displacement gradient, but not in the Eulerian equation. If we look a plane wave propagating in the x-direction, we should have $\partial_Y p, \partial_X U_j, \partial_Y U_i \approx 0$, and the two equations should yield similar behavior. But in the case of intersecting waves, the particle and material can vibrate in the y-direction, and the terms $\partial_Y U_j$ and $\partial_X U_j$ can become significant and effect the wave.

In the numerical experiment we want to investigate if this has any effect and significance on the scattered wave, and also how the scattered high frequency(HF) wave signal differs with and without the influence of the intersecting low frequency(LF) wave. To do this, we do three different simulations with both Lagrangian and Eulerian equations:

- HF: Only the high frequency wave, recording P^l_{HF} and P^e_{HF}
- LF: Only the low frequency wave, recording P^l_{LF} and P^e_{LF}
- LFHF Both low and high frequency wave, recording P^l_{LFHF} and P^e_{LFHF}

We use the exact same LF and HF wave sources in all simulations. The LF data is used to remove the LF signal from the LFHF signal, for better comparison with the HF signal, as seen in Figure 2. Using the parameters and sources given above, we simulate for a period $t_{sim} = 8 \cdot 10^{-6}$ s, set $t_m = \frac{1}{2} t_{sim}$, and choose a particle diameter of about 180 μm. We use a spatial apodization of the sources, i.e. we round off the source edges in a Gaussian fashion, to avoid unwanted numerical oscillations.

A plot of the intersecting waves can be seen in Figure 3. Next, we compare the relative difference in the signal for P^l_{HF} and P^l_{LFHF}, and the the relative difference in signals from different simulations with the Lagrangian and Eulerian equations. Plots of the results from the simulations can be seen in Figures 4-5.

[2]Where the Lagrangian density has been neglected.

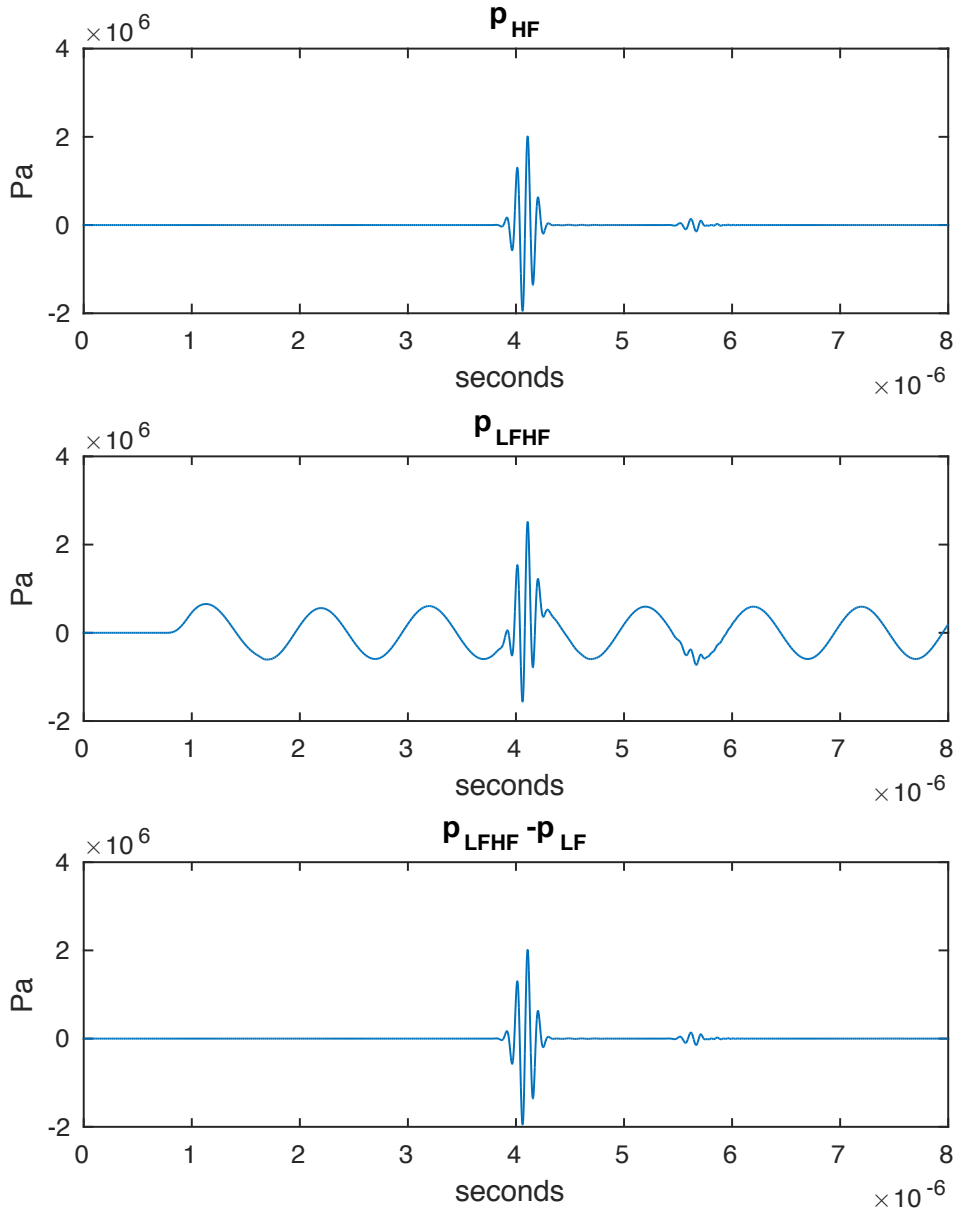

FIGURE 2. The recorded signal from simulations. The first plot shows the HF signal P^l_{HF} alone, the second shows the LFHF signal P^l_{LFHF}, and the third shows the LFHF signal when the signal from simulations with only the LF wave have been subtracted, i.e. $P^l_{LFHF} - P^l_{LF}$.

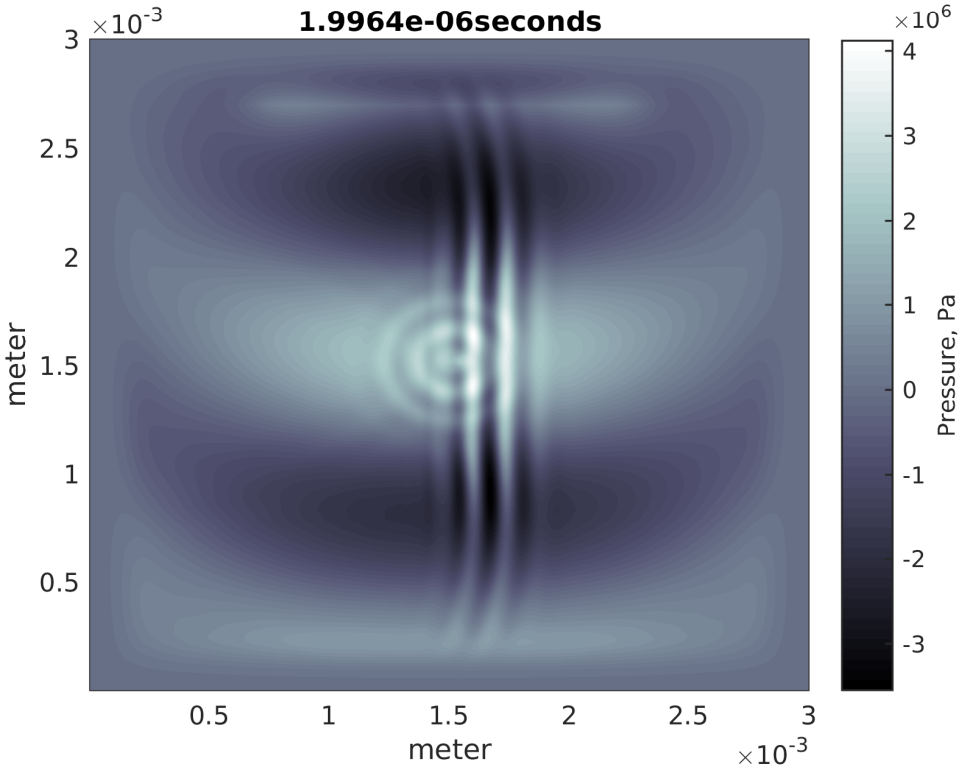

FIGURE 3. The high frequency wave coming in from the left, just as it hits the particle. The intersecting LF wave travels from the top and downwards. We also see the spherical waves from the scattering with the particle at the center.

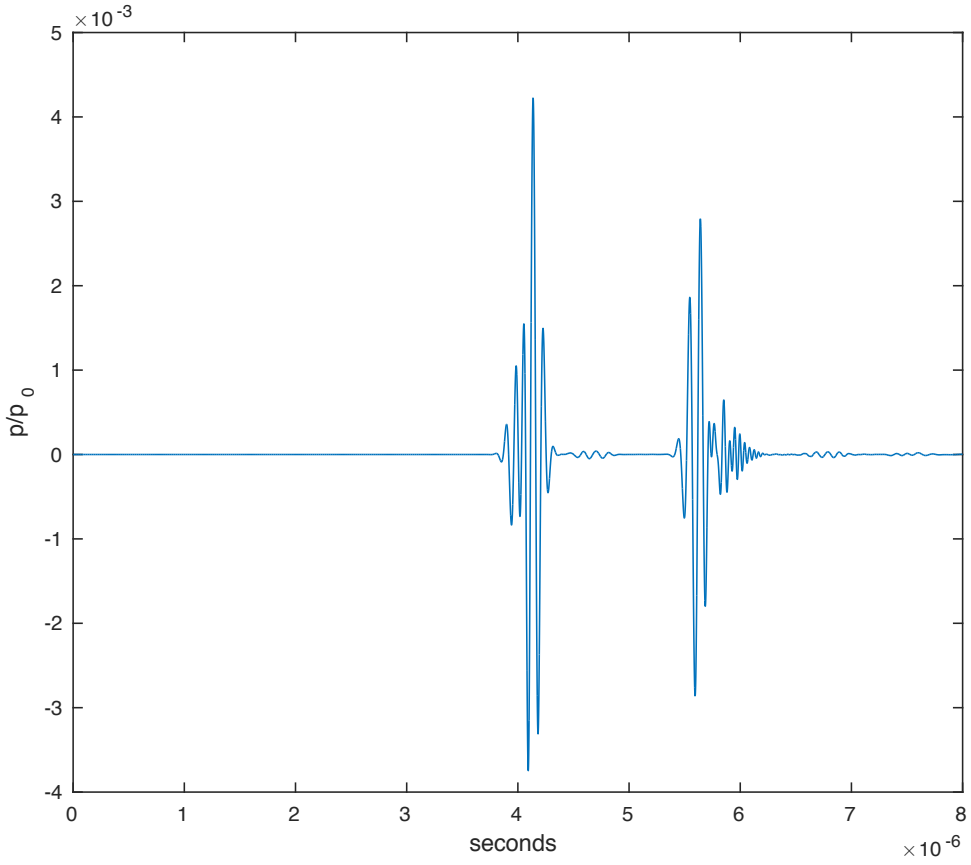

FIGURE 4. Plot of the relative difference in the recorded signals from the simulation with only the HF wave and the simulation with both LF and HF waves, $\frac{P^l_{HF}-(P^l_{LFHF}-P^l_{LF})}{p_0}$. The first peaks are from the outgoing wave, and the second peaks are from the scattered wave. We see that both the outgoing and reflected wave signals clearly differ, and that the difference in the scattered signal is larger than the outgoing signal, relative to the signal amplitudes seen Figure 2.

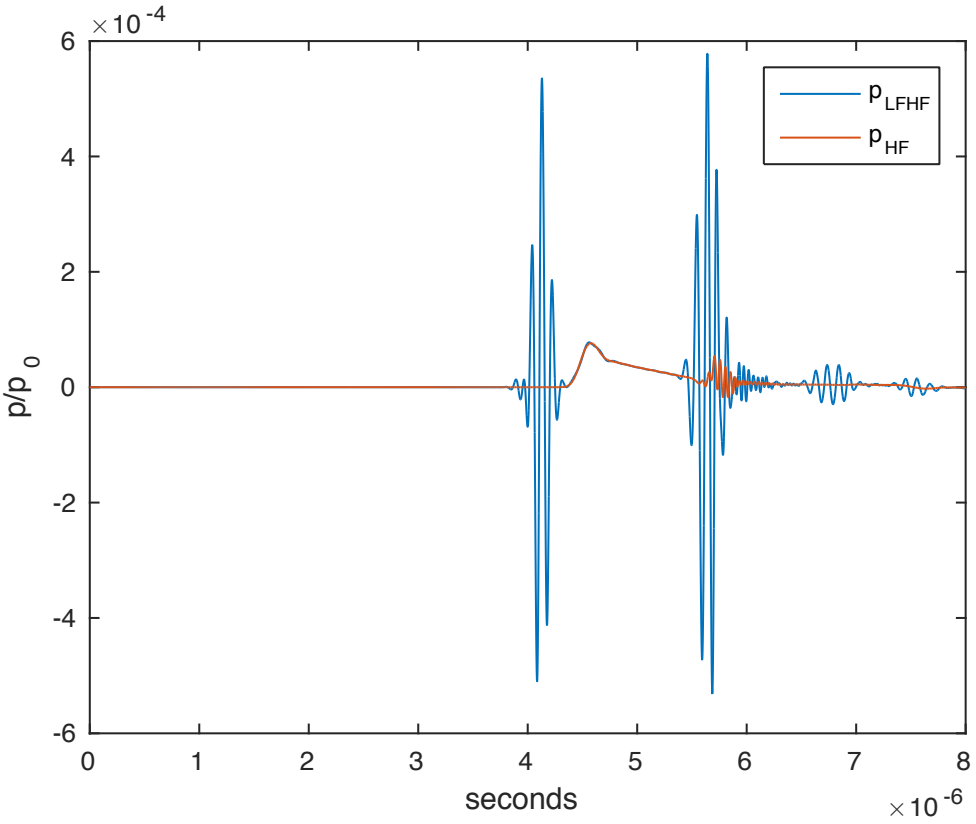

FIGURE 5. Plot comparing the relative difference in HF and LFHF signals obtained from simulations with the Lagrangian and Eulerian eqution. We compare $\frac{P^l_{LFHF}-P^l_{LF}}{p_0} - \frac{P^e_{LFHF}-P^e_{LF}}{p_0}$ to $\frac{P^l_{HF}-P^e_{HF}}{p_0}$. The relative difference is about a factor ten larger for the Lagrangian simulations. It is interesting to note that the difference in the outgoing signal is zero for P^e, but not for P^l. This can be explained by the variation in displacement caused by the intersecting LF waves, since this variation is only accounted for in the Lagrangian equation.

The results shows a small but clear difference in the received signal in the reflected wave when the intersecting LF wave is present. Figure 4 also shows that the difference is more significant in the Lagrangian equations than in the Eulerian equations. This indicates that the effects from the displacement variations accounted for in the Lagrangian equations can contribute in explaining the observations in the experiment by *Angelsen* and *Myhre*. These results can be important. If they can help to explain how a small calcium particle better can be detected, must be decided by others, preferably by linking experiments and simulations more closely and using signal processing.

Summary and further work

In this thesis we have investigated the equations governing acoustic waves. We have seen how the approximations in classical Eulerian formulation of these equations in some situations can be inaccurate. As an alternative to the Eulerian equations, we derived the Lagrangian equations, and pointed out why these equations are more suited to model waves in heterogeneous materials and in interaction with particles. We then investigated conservation of energy and energy attenuation, and showed how a frequency dependent viscoelastic attenuation term can be added to the Lagrangian equations. We continued to develop a second order numerical scheme to solve the Lagrangian equations, and did a numerical experiment using this scheme, where we also compared the Eulerian and Lagrangian equations.

If the work in this thesis should be taken further, it would be interesting to compare the results in Chapter 6 with experimental data, and to use a more powerful computer or a faster programming language, to be able to simulate larger computational domains and longer simulation times. One should also think of other scenarios where the Lagrangian equations could serve as a better model, e.g. in modeling micro bubbles or waves that interact with moving parts of the body. The numerical method should also be further analyzed, and implemented in parallel, and it would be interesting to develop a numerical scheme using a pseudospectral method [31]. It would also be interesting to further investigate the Lagrangian equations, especially the pressure equation (3.42).

Appendix

```
%%% NUMERICAL SCHEME FOR A 2-D NONLINEAR WAVE EQUATION %%%
%%% IN LAGRANGIAN COORDINATES USING A MODIFIED         %%%
%%% LEAPFROG-STAGGERED GRID SCHEME, AND IN EULERIAN    %%%
%%% COORDINATES USING A REGULAR LEAPFROG-STAGGERED GRID%%%
%%% SCHEME.                                           %%%


%grid spesification etc.
Lx=3000*10^-6;                  %x-length, meters
Ly=3000*10^-6;                  %y-length, meters
I=250;                          %x-steps
J=250;                          %y-steps
dx=Lx/I;                        %spatial increments
dy=Ly/J;
T=2*10^-6;                      %simulation time, seconds

%material parametres etc.
kappa_ambient=5.269*10^-10;     %background compressibilty
rho_ambient=9.28*10^2;          %background density
beta_ambient=6.14;              %nonlinearity parameter
rho_0=rho_ambient*ones(2*J,2*I);
kappa_0=kappa_ambient*ones(2*J,2*I);
beta=beta_ambient*ones(2*J,2*I);

% Field variables: pressure, displacement, velocity, etc.
% for both Lagrangian and Eulerian(marked pE, vE etc.) simulations
%pressure
p=zeros(2*J,2*I);
px=p;
py=p;
pE=zeros(2*J,2*I);
pxE=p;
pyE=p;

psource=p;
%displacement
u1=zeros(2*J,2*I);
u2=zeros(2*J,2*I);
%velocity
v1=zeros(2*J,2*I);
v2=zeros(2*J,2*I);
```

```
v1E=zeros(2*J,2*I);
v2E=zeros(2*J,2*I);
%boundary condition for v
yz=zeros(1,2*I);
xz=zeros(2*J,1);

%reference grid/lagrangian coordinates
[X,Y]=meshgrid(linspace(0,Lx,2*I),linspace(0,Ly,2*J));


%defining the heterogeniety/particle
rho_p=2.8;              %scaling factors for background density etc.
kappa_p=0.05;           %in the particle region
beta_p=0;
lx=8;                   %defining the size of the particle in
ly=8;                   %number of steps
Istart=ceil(I);         %position of the particle
Jstart=ceil(J);
% %Square particle
rho_0(Jstart:Jstart+ly,Istart:Istart+lx)=...
    rho_p*rho_0(Jstart:Jstart+ly,Istart:Istart+lx);
kappa_0(Jstart:Jstart+ly,Istart:Istart+lx)=...
    kappa_p*kappa_0(Jstart:Jstart+ly,Istart:Istart+lx);
beta(Jstart:Jstart+ly,Istart:Istart+lx)=...
    beta_p*beta(Jstart:Jstart+ly,Istart:Istart+lx);

%%Circular particle
% sx=ceil(I);
% sy=ceil(J);
% r=30;
%
% for i=1:I
%     for j=1:J
%         if( sqrt((i-sx)^2 + (j-sy)^2) ≤10)
%         rho_0(j,i)=rho_p*rho_0(j,i);
%         kappa_0(j,i)=kappa_p*kappa_0(j,i);
%         end
%     end
% end

%Triangualr particle
% H=20;
% for i=0:H
%     for j=i:H
%       rho_0(Jstart-j,Istart-i)=rho_p*rho_0(Jstart-j,Istart-i);
%       kappa_0(Jstart-j,Istart-i)=kappa_p*kappa_0(Jstart-j,Istart-i);
%       beta(Jstart-j,Istart-i)=beta_p*beta(Jstart-j,Istart-i);
%     end
% end

%time integration parameters
kappa_min=kappa_ambient*kappa_p;
CFL=.2;
```

```
c_max=sqrt(1/(kappa_min*rho_ambient));
dt=min(dx,dy)*CFL/c_max;
steps=ceil(T/dt);



%Construction of the PML
PML=zeros(2*J,2*I);
pml_sz=ceil(I/5);
pml_factor=10^8;
damp=pml_factor*(linspace(0,1,pml_sz)).^2;

for k=pml_sz:-1:1
    PML(k,k:end+1-k)=ones(1,2*I-2*(k-1))*damp(pml_sz+1-k);
    PML(k:end+1-k,k)=ones(1,2*I-2*(k-1))'*damp(pml_sz+1-k);
end

for k=1:pml_sz
    PML(end-pml_sz+k,(pml_sz-k+1):(end-pml_sz+k))=...
        ones(1,2*I-2*(pml_sz-k))*damp(k);
    PML((pml_sz-k+1):(end-pml_sz+k),end-pml_sz+k)=...
        ones(1,2*I-2*(pml_sz-k))'*damp(k);
end




%source conditions for exciting waves, frequencies etc
LF=1*10^6;
HF=10*10^6;
SW=1400*10^-6;                          %source width
SSW=200*10^-6;                          %apodization width
sigmaHF=(1/(.3*HF))/4.3;
sigmaLF=(1/(.5*LF))/4.3;
t_mLF=1/(.5*LF);
t_mHF=1/(.5*HF);
p_0=2*10^6;
z_0=(rho_ambient*sqrt(1/(rho_ambient*kappa_ambient)));
%source apodization to avoid unwanted oscillations
SA=apodization(SW,SSW,J,Ly);


t_mid=(1/2)*T;



for i=1:J;
    k(i)=2*i;
end


%received signal, comparison etc.

```

```
148 p_rec_mean=zeros(1,steps);
149 pE_rec_mean=p_rec_sum;
150
151 for n=1:steps
152
153
154   % imposing different boundary conditions/ pressure source
155
156  % v_sin_source_HF=2*(p_0/z_0)*sin(2*pi*HF*(n*dt-t_mHF))...
157  %*exp(-((n*dt-t_mHF)^2)/(2*sigmaHF^2))*SA;
158   v_sin_source_HFdelay=2*(p_0/z_0)*sin(2*pi*HF*(n*dt-t_mHF))...
159       *exp(-((n*dt-t_mid)^2)/(2*sigmaHF^2))*SA;
160  % v_sin_source_LF=-2*(p_0/z_0)*sin(2*pi*LF*(n*dt-t_mLF))...
161  %*exp(-((n*dt-t_mLF)^2)/(2*sigmaLF^2))*SA;
162  % v_sin_source_contHF=2*(p_0/z_0)*sin(2*pi*HF*(n*dt-t_mHF))*SA;
163   v_sin_source_contLF=2*(p_0/z_0)*sin(2*pi*LF*(n*dt-t_mLF))*SA;
164
165 % %
166   psource(:,pml_sz)=-v_sin_source_HFdelay;
167   psource(:,pml_sz+1)=psource(:,pml_sz);
168 % %
169    psource(end-pml_sz,:)=v_sin_source_contLF';
170    psource(end-pml_sz+1,:)=psource(end-pml_sz,:);
171
172
173
174  %Discrete operators for U
175  du2dy=(1/dy)*([u2(2:end,:);yz]-[yz;u2(1:end-1,:)]);
176  du1dx=(1/dx)*([u1(:,2:end),xz]-[xz,u1(:,1:end-1)]);
177  du2dx=(1/dx)*([u2(:,2:end),xz]-[xz,u2(:,1:end-1)]);
178  du1dy=(1/dy)*([u1(2:end,:);yz]-[yz;u1(1:end-1,:)]);
179
180
181  dpdx=(1/dx)*([p(:,2:end),p(:,end)]-[p(:,1),p(:,1:end-1)]);
182  dpdy=(1/dy)*([p(2:end,:);p(end,:)]-[p(1,:);p(1:end-1,:)]);
183  dpEdx=(1/dx)*([pE(:,2:end),pE(:,end)]-[pE(:,1),pE(:,1:end-1)]);
184  dpEdy=(1/dy)*([pE(2:end,:);pE(end,:)]-[pE(1,:);pE(1:end-1,:)]);
185
186  %Integration of v1,v2
187  v1=v1-(dt./rho_0).*((1+du2dy).*dpdx -du1dy.*dpdy) - (dt)*PML.*v1;
188  v2=v2-(dt./rho_0).*((1+du1dx).*dpdy-du2dx.*dpdx)  - (dt)*PML.*v2;
189  %Linear integration, Euler equations
190  v1E=v1E-(dt./rho_0).*dpEdx  - (dt)*PML.*v1E;
191  v2E=v2E-(dt./rho_0).*dpEdy - (dt)*PML.*v2E;
192
193  %Discrete operators for p, v1, v2
194  dv1dx=(1/dx)*([v1(:,2:end),xz]-[xz,v1(:,1:end-1)]);
195  dv2dy=(1/dy)*([v2(2:end,:);yz]-[yz;v2(1:end-1,:)]);
196
197  dv1Edx=(1/dx)*([v1E(:,2:end),xz]-[xz,v1E(:,1:end-1)]);
198  dv2Edy=(1/dy)*([v2E(2:end,:);yz]-[yz;v2E(1:end-1,:)]);
199
200  V1=(1/4)*([v1(:,2:end),xz]+[xz,v1(:,1:end-1)]...
```

```
      +[v1(2:end,:);yz]+[yz;v1(1:end-1,:)]);
 V2=(1/4)*([v2(:,2:end),xz]+[xz,v2(:,1:end-1)]...
      +[v2(2:end,:);yz]+[yz;v2(1:end-1,:)]);

 %Integration of p, u1, u2
 px=px-dt*Kinv(kappa_0,beta,p).*(dv1dx-.5*(1/dx)*psource)-(dt)*PML.*px;
 py=py-dt*Kinv(kappa_0,beta,p).*(dv2dy-.5*(1/dx)*psource)-(dt)*PML.*py;
 p=px+py;

 pxE=pxE-dt*Kinv(kappa_0,beta,pE).*(dv1Edx-.5*(1/dx)*psource)-(dt)*PML.*pxE;
 pyE=pyE-dt*Kinv(kappa_0,beta,pE).*(dv2Edy-.5*(1/dx)*psource)-(dt)*PML.*pyE;
 pE=pxE+pyE;

 u1=u1+dt*V1;
 u2=u2+dt*V2;


 p_rec_mean(1,n)=mean(p((J-20):(J+20),pml_sz+20));
 pE_rec_mean(1,n)=mean(pE((J-20):(J+20),pml_sz+20));

%plotting
if mod(n,20)==0
      x=X+u1;
      y=Y+u2;
%
%
       pcolor(x(k,k),y(k,k),p(k,k));
       xlabel('meter')
       ylabel('meter')
      shading interp;
      colormap('bone')
%        plot(x(J,k),p(J,k))
     title(strcat(num2str(n*dt),'seconds'))
      h=colorbar;
      ylabel(h,'Pressure, Pa')
     drawnow


end

end


%Apodization function
function [ pB ] = apodization(Cw,Sw,J,Ly)

smoothJ=ceil(2*J*Sw/Ly);
sourceJ=ceil(2*J*Cw/Ly);
smooth2=[.5*(1+sin(linspace(-pi/2,pi/2,smoothJ))),ones(1,sourceJ)...
    ,.5*(1+cos(linspace(0,pi,smoothJ)))];
l=length(smooth2);
pB=zeros(1,2*J);
pB(1,(J-ceil(l/2)):(J+floor(l/2))-1)=smooth2';
```

```
254
255
256 end
257
258 %Kinv function
259
260 function [ dK_inv ] = Kinv(kappa_0,beta,p)
261
262 dK_inv=1./(kappa_0 -2*beta.*kappa_0.^2.*p);
263
264 end
```

Bibliography

[1] Aanonsen, S.I., Barkve, T., Tjøtta, S., Naze Tjøtta, J., *Distortion and harmonic generation in the nearfield of a finite amplitude sound beam*, J. Acoust. Soc. Am. 75, 749, 1984.

[2] Adams, R.A., Essex, C., *Calculus: A Complete Course*, Person, Harlow, 2013.

[3] Angelsen, B.A., *Detection of μC particles in soft tissue*, DMF-ISB, NTNU, Trondheim, 2015.

[4] Angelsen, B.A.J., *Ultrasound Imaging Vol. 1 & Vol 2*, Emantec, Trondheim, 2001.

[5] Berenger, J.-P., *A Perfectly Matched Layer For The Absorption Of Electromagnetic Waves*, Centre d'analyse de Défense, France, 1994.

[6] Beyer, R.T., *Nonlinear Acoustics*, Naval Ship Systems Command, Department of the Navy, 1974, Rhode Island.

[7] Blackstock, D.T., *Fundamentals of Physical Acoustics*, John Wiley & Sons, Inc., New York, 2000.

[8] Cobbold, R.S.C., *Foundations of Biomedical Ultrasound*, Oxford University Press, New York 2007.

[9] Cox, B., *Acoustics for Ultrasound Imaging*, Lecture Notes, University College London, 2013.

[10] Demi, L., Verweij, M.D., *Nonlinear Acoustics* , Comprehensive Biomedical Physics, Elsevier, Amsterdam, 2014.

[11] Feynman, R.P., Leighton, R.B., Sands, M *Feynman Lectures on Physics*, Vol II, California Institute of Technology, California, 2010.

[12] Fletcher, N.H., *Nonlinear Dynamics and Chaos in Musical Instruments*, C.S.I.R.O., Australia, 1993.

[13] Griffiths, G.W., Schiesser, W.E., *Linear and Nonlinear waves* `http://www.scholarpedia.org/article/Linear_and_nonlinear_waves`

[14] Haddad, Y.M., *Viscoelasticity of Engineering Materials*, Chapman & Hall, London, 1995.

[15] Hamilton, M.F., Blackstock, D.T., *Nonlinear Acoustics*, ACADEMIC PRESS, San Diego, CA, 1997.

[16] Holmes, M.H., *Introduction to the Foundations of Applied Mathematics*, Springer Science+Business Media, LLC 2009

[17] Huijssen, J., *Modeling of Nonlinear Medical Diagnostic Ultrasound*, PhD-thesis, Delft University of Technology, Netherlands, 2008.

[18] Jing, Y., Cleveland, R.O., *Modeling the propagation of nonlinear three-dimensional acoustic beams in inhomogeneous media*, J. Acoust. Soc. Am. 122, 1352, 2007.

[19] Landau, L.D., Lifshitz, E.M., *Theory of Elasticity*, Institute of Physical Problems, USSR Academy of Sciences, Moscow, USSR(!), 1986.
[20] Leeman, S., Jones, J., *Visco-Elastic Models for Soft Tissue*, Springer, Netherlands, 2009
[21] Liu, Q.-H., Tao, J. *The perfectly matched layer for acoustic waves in absorptive media*, Klipsch School of Electrical and Computer Engineering, New Mexico State University, Mexico, 1997.
[22] Oden, J.T., *An Introduction to Mathematical Modelling*, John Wiley & Sons, New Jersey, 2011.
[23] Qi, Q., Geers, T. L., *Evaluation of the Perfectly Matched Layer for Computational Acoustics*, Center for Acoustics, Mechanics and Materials, Department of Mechanical Engineering, University of Colorado, Colorado, 1996.
[24] Raviart, P-A., Godlewski, E., *Numerical Approximation of Hyperbolic Systems of Conservation Laws*, Springer-Verlag, New York, 1996.
[25] Rienstra, S.W., Hirschberg, A., *An Introduction to Acoustics*, Eindhoven University of Technology, 2015, `http://www.win.tue.nl/~sjoerdr/papers/boek.pdf`.
[26] Salsa, S., *Partial Differential Equations in Action*, Springer-Verlag, Italia, 2008.
[27] Strikwerda, J.C., *Finite Difference Schemes and Partial Differential Equations*, SIAM, California, 2004.
[28] Thomas, D.C., *Theory and Estimation of Acoustic Intensity and Energy Density*, Brigham Young University, Provo, 2008.
[29] Treeby, B.E., Jaros, J., Rendell, A.P., Cox, B.T., *Modeling nonlinear ultrasound propagation in heterogeneous media with power law absorption using a k-space pseudospectral method*, Acoustical Society of America, 2012.
[30] Varslot, T., Måsøy, S-E., *Forward propagation of acoustic pressure pulses in 3D soft biological tissue*, Modeling Identification and Control, vol.27, no.3, pp. 181–200, 2006.
[31] Verweij, M.D., Treeby, B.E., van Dongen, K.W.A., *Simulation of Ultrasound Fields*, Comprehensive Biomedical Physics, Elsevier, Amsterdam,2014
[32] Yee, K., *Numerical solution of initial boundary value problems involving Maxwell's equations in isotropic media*, Antennas and Propagation, IEEE Transactions vol 14.3, 1966.